
Species sympatry shapes brain size evolution in Primates

Benjamin Robira^{1,2,*}

Benoît Perez-Lamarque^{3,4}

¹ Centre d'Écologie Fonctionnelle et Évolutive, Université de Montpellier & CNRS, Montpellier, France.

² Anthropologie et Ethnobiologie, Centre National de la Recherche Scientifique/Muséum National d'Histoire Naturelle, University Paris Diderot, Sorbonne Paris Cité, Musée de l'Homme, Paris, France.

³ Institut de Biologie de l'École Normale Supérieure (IBENS), École Normale Supérieure, CNRS, INSERM, Université PSL, Paris, France.

⁴ Institut de Systématique, Évolution, Biodiversité (ISYEB), Muséum National d'Histoire Naturelle, CNRS, Sorbonne Université, EPHE, Université des Antilles, Paris, France.

* Correspondence: [Benjamin Robira <benjamin.robira@normalesup.org>](mailto:benjamin.robira@normalesup.org)

Abstract | Main hypotheses related to animal intelligence evolution highlight the role of conspecifics. Yet, space is a place often occupied by many species, sometimes belonging to the same ecological guild. These sympatric heterospecifics can act as competitors or cooperators, thereby stimulating cognition. They can also contribute to modifying and depleting the environment, making it poorly predictable and thereby alleviating the benefit of cognition. Considering brain size as a proxy for cognition, we used primates to test for the intertwine between species sympatry and cognition, and retraced the evolutionary history of several brain areas considering competitive or non-competitive evolutionary scenarios. We found that competitive evolutionary scenarios best predicted the evolution of brain areas related to interacting with the social or ecological environment, with a decrease of their relative size the higher the sympatry rate, but not of the whole brain or brain areas used in immediate information processing. Moreover, sympatry negatively affected primate diversification which was unrelated to the size of brain areas. Overall, this comparative study suggests that species sympatry, which likely convolutes the environment, contributes to shaping the selective pressure acting upon primate cognition and diversification.

❖ **Keywords:** Brain size - Cognition - Competition - Co-occurrence - Diversification - Intelligence evolution - Primates - Sympatry

📄 **Word Count:** 5911

Introduction

Cognition evolution results from the balance between socio-ecological drivers promoting cognitive abilities¹ and physiological and energetic constraints². Primates are pivotal species for cognitive studies³ because their cognition is thought to be promoted by interactions of individuals with conspecifics within the social unit^{4,5}, among generations^{6–11}, between social units¹², or with the rest of their environment^{13–15}. However, space is a place often occupied by many species belonging to the same ecological guild and we can predict that such interactions with sympatric heterospecifics are likely to strongly shape the evolution of cognition.

Retracing the evolutionary history of cognitive abilities proves to be challenging because there is still no consensual measurement applicable across all species. Up to now, a raw approximation consists in considering brain size as a proxy for cognitive abilities (but see discussion in Logan *et al.* [16]). Yet, the brain is a mosaic of areas cognitively specialized¹⁷ and these areas are likely to be differently affected by species sympatry. For instance, the Striatum is stimulated during social interactions¹⁸. Its size is thus expected to be positively influenced when contacts with other species increase, as in species performing mixed-species groups, which is nonetheless rather infrequent in primates (but see callitrichine primates in particular, Heymann & Hsia [19]). The Striatum also underpins reward expectation and action, goal-directed behaviour and planning abilities²⁰ which is key when foraging. Other foraging-related areas, as the Main Olfactory Bulb (MOB) or the Hippocampus, home of a spatio-temporal memory²¹, are also expected to be influenced by the ecological environment. Such areas are thought to be particularly important for frugivorous primates, as fruits are the archetype of a hard-to-find resource yet predictable^{22,23}, and larger areas, taken as equivalent to more advanced cognitive abilities, might be more advantageous. Similarly, more generally-used areas, such as the Cerebellum^{24,25} and the Neocortex²⁶ underlying movement and/or general information processing and retention, could also be stimulated by the presence of other species movement traces, noises or odors to decode. To sum up, a first possibility is that sympatric heterospecifics could altogether stimulate cognition and promote larger sizes of the brain areas related to interacting with the social or ecological environment.

However, if the changes induced by sympatric species increases the environmental unpredictability too much, sympatry could on the contrary change the selective pressure applying to cognitive abilities²⁷. Indeed, due to the cost of maintaining the brain functional²⁸, it is expected that the increase in environmental unpredictability only stimulates cognition up to a certain threshold (i.e. positive selection for bigger brain), before smaller brain sizes of foraging-related areas become more adaptive (because costs are no longer compensated by the benefit of memory). Similarly, it is possible that processing heterospecifics cues, and other environmental cues (e.g. phenology cues) might not necessitate the same cognition level, with the former being potentially simpler to process (since relying on easily accessible social cues) than the latter (relying on trial-and-error processes and personal experience of potentially elusive environmental cues)²⁹. In this case, the size of brain areas involved in immediate information processing should be less large in sympatric than in non-sympatric conditions. To sum up, a second possibility is that sympatric heterospecifics could hamper the benefits of cognition on foraging, and thus slowdown brain size increase. In an extreme

case, it could even induce positive selection for smaller brain size.

Here, we investigated the intertwine between species sympatry and cognition using frugivorous primates as study example. To infer the effect of species interactions on brain size evolution within frugivorous primates, we evaluated support for competitive or non-competitive evolutionary scenarios, accounting or not for sympatry, and investigated the directionality of the selection induced by sympatry history upon brain size evolution. Finally, we tested for correlative patterns between the evolutionary success (species diversification) in primates with brain size or current sympatry context.

Results

We gathered a large database on the whole brain size, the size of the Cerebellum and the Neocortex, involved in daily information processing and retention, and the Main Olfactory Bulb (MOB), the Striatum, and the Hippocampus, those three latter being related to social and foraging-related tasks, containing between 34 to 182 frugivorous primate species (depending on the brain area considered). It evidenced ample variations in brain size. For instance, the lemuriformes, that are known to prioritize smell compared to other primate species, have the largest relative MOB size (i.e. pondered by whole-body mass) in our data (Lemuriformes: mean \pm SE = 0.23 ± 0.07 , other: 0.12 ± 0.04 , 3). Similarly, platyrrhini, and callitrichine primates in particular, are known to form poly-specific associations³⁰ and indeed show the highest relative size of the Striatum in our data (Platyrrhini: mean \pm SE = 0.91 ± 0.07 , other: 0.59 ± 0.07 , 3).

We first reconstructed primate biogeography history ($N_{species} = 214$, Matzke [31]; Matzke [32]) when considering 12 biogeographic areas (Figure 1; Kamilar [33]) and their diet evolution ($N_{species} = 192$ to 269; Bollback [34]). We then calculated the likelihoods of models considering the role of species interactions (matching competition MC models, Nuismer & Harmon [35]; models of linear or exponential density dependence, DD_{lin} and DD_{exp} , of the evolutionary rate on the number of sympatric lineages; Drury *et al.* [36] see [Models of trait evolution: does interspecific interactions shape brain size evolution?](#)) in the evolution of either the whole brain (using the encephalic quotient, EQ, as a proxy), or the size of the aforementioned specific brain areas relative to the whole-body mass (Figure. 3) and compared their likelihood to those of simpler models assuming no effect of species interactions, like the Brownian Motion (BM), the Ornstein-Uhlenbeck process (OU) considering that traits are constrained around on optimal value (e.g. stabilizing selection; see Blomberg *et al.* [37] for a review) or the Early-Burst model (EB, Blomberg *et al.* [38]), this latter allowing to check for a time-dependence of the evolutionary rate, hence emphasizing that, if any, the density effect is not an artefact due to time-dependence. Support for each model was evaluated using an information-theoretic framework³⁹ based on the weights of the Akaike Information Criteria corrected for small samples (AICc) when considering all six models (MC, DD_{lin} , DD_{exp} , BM, OU, EB, see [Models of trait evolution: does interspecific interactions shape brain size evolution?](#)).

We found that non-competitive models were the most likely in describing the evolutionary history of the EQ, the Neocortex, and the Cerebellum (Figure 3 and 4), two areas specifically involved in movement and/or general information processing^{24–26} but also in memory

consolidation for the Neocortex²⁶. The fact that these biggest areas are best described by the Ornstein-Uhlenbeck process suggests a stabilization towards an optimal size and illustrates the trade-offs between costs and benefits of brain development⁴⁰. By contrast, competitive models were most supported in foraging-related and social areas, either specialised in spatio-temporal memory (Hippocampus, Burgess *et al.* [21]) or planning abilities and reward assessment (Striatum, Báez-Mendoza & Schultz [18]; Johnson *et al.* [20]), and tended to be so for one brain area involved in sensory abilities (the main olfactory bulb, MOB; Figure 3 and 4). When density-dependent models were the best fit, the rate (r , Figure 4) suggested an acceleration of the evolutionary tempo together with increased lineage diversity for the Hippocampus and the Striatum, but a slowdown for the MOB.

Next, to understand the directionality of the selection gradient shaped by sympatry (i.e. selection for “bigger” or “smaller” brain the more species), we fitted phylogenetic regressions (see [Phylogenetic regressions](#) a)). For these linear regressions, the predicted variable was the relative brain size values of the different areas. We considered the average surface of the frugivorous species range that was overlapped by other sympatric frugivorous species, as well as the number of such sympatric frugivorous species across their entire distribution range as covariates based on IUCN data⁴¹. On average (\pm SE), the considered primate species had 52% of their range overlapping with other species (\pm 2). That ranged from 0% of overlap (*Macaca nigra*), to 100% of overlap (*Cercopithecus pogonias*, *Alouatta pigra*, *Loris tardigradus*, *Hylobates moloch*, *Cercocebus galeritus*, *Presbytis melalophos*, *Semnopithecus entellus*). In terms of distribution range, the considered primate species co-occurred on average with 6.38 other primate species (\pm 0.39), ranging from 0 other species (*Daubentonia madagascariensis*, *Eulemur coronatus*, *Eulemur fulvus albifrons*, *Macaca cyclopis*, *Macaca fuscata*, *Macaca nigra*, *Macaca tonkeana*, *Miopithecus talapoin*), to 21 species (*Galagoides demidoff*). The number of sympatric species never influenced significantly the relative size of the brain or other specific areas (Table 1). Conversely, we found that the percentage of range shared with other species correlated with the relative size of areas that were better fit with competitive models: the Hippocampus, and the Striatum (Hippocampus: $t = -1.94$, $p = 0.058$; Striatum: $t = -2.26$, $p = 0.028$). The correlations were all negative (Hippocampus: est. = -0.39, CI95% = [-0.76,-0.01]; Striatum: est. = -0.4, CI95% = [-0.77,-0.04]), which means that higher species overlap associates with lower relative size, insensitive to data and phylogenetic uncertainty (Table S1, Figure S8). Thus, it suggests that sympatric species are either subject to a positive selection towards smaller brain, or to a less intense selection for advanced cognitive abilities compared with isolated species.

In addition, we investigated the evolutionary consequences of brain evolution and sympatry by evaluating whether brain sizes and sympatry level correlated with species diversification rates (i.e. speciation minus extinction rates), by using lineage-specific birth-death models of species diversification^{42,43}. Overall, species diversification, estimated based on molecular phylogeny increased over time (Figure S4), particularly in the early and late Miocene, around 25.06 (CI95% = [24.77,25.36]) and 11.04 (CI95% = [10.74,11.34]) Myr ago (Figure S4). When accounting for phylogenetic dependence, no significant relationship between diversification rate and the relative size of brain areas was found (Table 2, Figure S8; see robustness in Table S2). Given the context dependence of the direction of selection (towards bigger sizes in the absence of other species, smaller sizes otherwise), there is no surprise that we do not observe a correlation between evolutionary success (approximated by diversification rate) and the three

studied areas affected by inter-species sympatry. Surprisingly however, we found no positive association between the EQ and the diversification rate, nor of that latter with the relative size of the Cerebellum or the Neocortex, two areas insensitive to inter-species sympatry too. This is puzzling because this contradicts a recent study⁴⁴. The visual inspection of the regressions however clearly evidenced a positive trend for the EQ and the Neocortex if discarding phylogenetic non-independence (Figure S6). In fact, a sudden encephalisation in primates is clearly associated to a limited number of closely-related species^{44,45}. This clearly limits the statistical power of our phylogenetically corrected analyses as we cannot decipher whether the connivance between brain size and evolutionary success results from a true biological link or appeared by chance. A positive association between brain size and diversification was also found in birds⁴⁶ given that bigger brains act as a buffer to environmental challenge, thus boosting individuals' fitness⁴⁷. This means that, despite what we found here, the positive association between brain size and evolutionary success evidenced in Melchionna *et al.* [44] remains a likely possibility. Finally, although diversification was uncorrelated with brain size in frugivorous primates, it was influenced by the sympatry context. In particular, phylogenetic regressions highlighted a negative effect of the number of sympatric species on the diversification rate (est. = -5.04e-03, CI95% = [-0.01, 1.34e-04], $t = 2.56e-03$, $p < 0.001$, Table 3, Figure S8). In other words, the higher the number of sympatric species, the lower the diversification, a trend that is frequently suggested in many tetrapod clades⁴⁸, but which stands as an inverted pattern compared to what is found in New World passerines⁴⁹.

Discussion

The bigger is not necessarily the better. The size of the brain is subject to a compromise between the energy it incurs, and the increase of fitness it allows. This is clearly emphasized by the fact that the biggest areas, the Cerebellum and the Neocortex, as well as the whole brain (EQ) were best described by the Ornstein-Uhlenbeck process, what might suggest a stabilisation towards an optimal size as a result of an equilibrium between costs and benefices. As the brain area is regionally specialised¹⁷, brain regions could be under different selective pressures as suggested by the differences we highlighted in some brain areas (e.g. MOB or Striatum) across different primate genera. Here, we further show that sympatry is one factor that affects the selective regime under which each brain region evolves: although the brain as a whole was insensitive to species sympatry, this latter nonetheless induced a change in the relative size of the Hippocampus, and the Striatum, and potentially in the MOB of frugivorous primates. These areas are involved in individual-based and social-based information processing, pinpointing that the two components might be under selection in primates^{1,45,50}. Overall, the relative sizes of foraging-related brain areas were negatively associated with one index of sympatry intensity (the range overlap with other species) and might thus be a consequence of direct or indirect interspecific interactions. In general, competition is the first-thought mechanism to describe community structures⁵¹. In primates, it is rare to observe direct competition between species, which should translate into site exclusion. In fact, inter-species site exclusion in this taxon has only been observed in gibbons⁵². For species with overlapping diet, indirect competition for resources might happen. It has

been shown that individuals tend to use social or environmental cues depending on their reliability^{53,54}. The utilization of these cues should promote cognition until reaching a certain range of environmental complexity^{27,55}. Our results could thus suggest that species sympatry may trigger an important decrease in cues reliability, for instance due to higher and unforeseen depletion rate. That would explain a relaxed positive selection for advance cognitive abilities, and conversely, given the cost of brain maintenance²⁸, would induce a negative selection towards the sizes of areas involved in foraging-related activities like the Hippocampus, the MOB and the Striatum. Not only was brain evolution affected by sympatry, but sympatry (the maximum number of co-occurring species only) induced a slowdown in diversification, which contrasts with the picture offered by passerine birds at finer resolution⁴⁹. Density-dependence within clade is often thought to lower diversification rate⁵⁶. In particular, species competing for resource are thought to contribute to limiting competitors' range⁵⁷, hence to constrain population size and diversification rate⁵⁸. Given the large resolution and low overlap threshold to consider sympatry considered here (i.e. overlap of 10% of the distribution area), this competitive view fits the observed influence of sympatry on frugivorous primate diversification.

The use of brain size as a proxy for cognition is a central debate with no optimal solution (see grounded criticism from Deaner *et al.* [59]; Healy & Rowe [60]; Logan *et al.* [16]). The current flourishing of consortia, allowing for much more detailed and standardized anatomical measurements (e.g. in primates: Milham *et al.* [61]), or with standardized behaviourally explicit comparisons (e.g. on captive⁶² or wild⁶³ primates), might alleviate biases stemming from brain size analysis, but this will take time to generate large-enough datasets. In the meanwhile, brain size is a proxy much appreciated in practice, because of its easy accessibility for a “large” number of species. Here, we showed that species sympatry is an important factor shaping the evolutionary history of animals' brain, but the proximate mechanisms at play remain to be elucidated. Finally, it is very likely that any hypothesis on cognition evolution, generally discussed within species, could be broadened to a between-species context: polyspecific social associations do exist⁶⁴, as well as inter-species territory defense^{65,66} or imitation and copying^{67,68}. As Alice said “It’s a great huge game of chess that’s being played—all over the world” (Carroll [69], Chapter II) and all individuals are just pieces to play with or against, no matter the species.

Methods

Data processing, analyses, and plots were computed with R software⁷⁰. Used codes and data are freely available at https://github.com/benjaminrobira/Temporal_memory_and_for_aging_efficiency. Note that in all these analyses, we discarded *Homo sapiens* and *Macaca sylvanus*, this latter being too geographically isolated. A summary of available data per species is presented in Appendix Figure 1.

Data Collection

Phylogeny

We used a block of chronogram trees of the primate taxon of the 10kTrees project (downloaded on the 11/05/2021, version 3), as well as a consensus tree of 1000 trees for the subsequent phylogenetic analyses. The trees contain 301 primate species.

Trait data

Brain data were obtained from DeCasien & Higham [71] for whole brain and all mentioned other parts (Cerebellum, Hippocampus, Main Olfactory Bulb (MOB), Neocortex, Striatum), Powell *et al.* [50] and Powell *et al.* [72] for whole brain, Cerebellum and Neocortex size, Todorov *et al.* [73] for Hippocampus and Neocortex size, Grueter [74] for the whole brain size and Navarrete *et al.* [75] for the whole brain, Cerebellum, Hippocampus and Striatum size. They were freely available in the main manuscript or supplementary materials. When a species was represented multiple times within dataset, we obtained a unique attribute by averaging it. From the global endocranial brain volume, we obtained the Encephalization Quotient (EQ, $N_{EQ,max} = 182$) as follows⁴⁵

$$EQ = 1.036 \times \text{Brainvolume} / (0.085 \times \text{Bodymass}^{0.775})$$

with the brain volume in cm^3 , 1.036 g/cm^3 being the assumed homogeneous brain density, and the body mass in g. EQ indicates whether the brain size ranges above (> 1) or below (< 1) expected given the body mass. Body mass was obtained from DeCasien *et al.* [45], Powell *et al.* [50], Grueter [74] and Pearce *et al.* [76]. The sub-parts of the brain were chosen because they were involved in immediate sensory information processing (MOB, $N_{MOB,max} = 39$), in movement and/or general information processing and retention (Neocortex, $N_{Neocortex,max} = 69$, Wiltgen *et al.* [26]; Cerebellum, $N_{Cerebellum,max} = 70$, Koziol *et al.* [24]; Sokolov *et al.* [25]), short-term working memory and long-term spatio-temporal memory (Hippocampus, $N_{Hippocampus,max} = 63$, Burgess *et al.* [21]). The Striatum ($N_{Striatum,max} = 63$) supports information processing during social interaction, reward assessment, planning or goal-oriented behaviours^{18,20}. To investigate their evolutionary history, we used the ratio between their volume and body mass, so as to maximize comparability. As such, the use of specific region size relatively to the body mass and not raw size depicts the evolution of cognitive abilities in terms of allocation rather than abilities per se (but see discussion in Deaner *et al.* [59]). Percentage of frugivory and/or folivory was obtained based on freely available dataset from

DeCasien *et al.* [45] and Powell *et al.* [50] for the frugivory and folivory rate, or Willems *et al.* [77] for the folivory rate.

Ranging Data

Current geographic (maximal possible) range of each primate species was assessed using ranging maps provided by the IUCN red list⁴¹. Ranging data were available for 249 species among the 301 represented in the 10kTrees primate phylogeny.

Primate species sympatry

One to multiple large-scale geographic areas were assigned to each species as soon as the species current distribution range overlapped in surface at 10 (low threshold) or 30% (high threshold; the maximum was chosen to 30% because on present data, a species could occupy as far as three areas, Figure 1). Overlap was calculated with the “gIntersection” function from the *rgeos* package⁷⁸ applied to Mercator-projected data to get the overlap contour, and the “area” function from the *geosphere* package⁷⁹, applied directly on unprojected longitudinal-latitudinal data for area size calculation. Based on the structure (i.e. number of species and their phylogenetic relationship) of primate communities at different field sites, Kamilar [33] determined clusters of sites with highly similar community structures that were shaped by both the environment geography and climatic correlates. We used this classification and manually mapped the geographic areas using Google earth professional (v7.3.3). These geographic areas are represented in Figure 1 and correspond to Central America, the North and the South of South America respectively, West Africa, Central Africa, and East/South Africa, East and West of Madagascar respectively, West Asia, Central/East Asia, South Asia and the Asian Islands. The chosen scale for the areas is large because (i) retracing history of a large number of areas necessitates considerable computational means. In addition, this drastically increases computational time of phylogenetic model of brain trait evolution too. Furthermore (ii), all species and particularly primate species suffer(ed) from recent extinction⁸⁰, with reduction of ranging areas at an unprecedented speed rate. Finer geographic characterization would therefore give too much weight to such anthropogenic effect that recently altered species distribution (e.g. evidenced on the North American fauna in Pineda-Munoz *et al.* [81]).

We retraced the history of the lineage ranges based on current observations of species range using the *BioGeoBEARS* package³¹, using the biogeographic stochastic mapping algorithm³². We fitted non-time-stratified dispersal-extinction-cladogenesis (DEC) models specifically suiting analyses of range data since it accounts for spatially explicit processes of cladogenetic and anagenetic events (see Matzke [31] for further details on these events). To reconstruct the evolution of species range, we fixed the maximum numbers of areas that could be occupied by a lineage at one time to three areas. A too high number of areas that can be occupied simultaneously drastically increases computational time. Here, we therefore chose that a species can at most occupy three areas since it offers the possibility to occupy a complete mainland continent. Finally, because these history reconstructions are likely to vary, for each run of DEC models (considering both possible overlaps to consider species presence), we obtained 10 stochastic maps that were all used in subsequent phylogenetic model fits (see

Phylogenetic models) to account for uncertainty of these ancestral range estimations (see Models of trait evolution: does interspecific interactions shape brain size evolution? (b)).

Dietary guild

We classified species as either “frugivorous” or “folivorous” based on the availability of frugivorous rate and folivorous rate, prioritizing frugivory over folivory. First, a species would be classified as frugivorous if the frugivory rate was at least above 20 (low threshold) or 40% (high threshold). If this was not the case, or frugivory rate was unavailable, a species could be classified as folivorous if the folivory rate was at least above 40 (low threshold) or 60% (high threshold). Otherwise, DeCasien *et al.* [45] gave a binary classification of diet, species being categorized as frugivorous or folivorous, partly based on anatomical criteria. Whenever the rate was not available, we referred to this classification. In any other cases, the species was discarded.

Frugivory rate was prioritized over folivory because we considered that since fruits are a highly palatable food source, it would be the key item that drives the foraging strategy (and associate consequence(s) on brain selection), even if less consumed. Additionally, to consider frugivory, we used a lower rate than for folivory for two reasons. First, such static rate does not reflect potential seasonality in fruit eating (e.g. Masi *et al.* [82]), which is generally shorter, hence a lower overall frugivory rate. Second, frugivory rate is likely to be underestimated in part because primates generally spend more time feeding on leaves than fruits, while rates are often based on relative feeding time, or observation frequency at the individual or group unit of feeding events. Finally, the methodology to obtain this rate could additionally vary (e.g. in addition to the two aforementioned estimations, one could also rely on the proportion of species targeted for their fruits/leaves). For all these reasons, we used two threshold levels (low, 20%, or high, 40%) to classify a species as frugivorous, as well as two threshold levels (low, 40%, or high, 60%) to classify a species as folivorous.

Considering diet as a binary variable (frugivory versus folivory), we retraced the evolutionary history of such discrete traits based on a continuous Markovian process (extended Mk models) and relying on a Bayesian approach³⁴, using the “simmap” function of the *phytools* package⁸³ and internally estimating the prior probability of trait (i.e. at the root) but with no prior on the transition matrix. Again, the obtained character history is in no case certain. Therefore, for each run, we obtained 10 stochastic character maps that were used in subsequent phylogenetic model fits [Phylogenetic models](#) to account for uncertainty of these ancestral diet estimations (see [Phylogenetic models, Models of trait evolution: does interspecific interactions shape brain size evolution?] (b)).

Phylogenetic models

Models of trait evolution: does interspecific interactions shape brain size evolution?

(a) Fitting models of trait evolution

We focused only on frugivorous primates, because sample size was otherwise insufficient,

and fitted phylogenetic models of EQ - or relative size of a specific brain area – evolution with and without species competitions. Models were fitted on different sample sizes due to non-availability of some data for some traits. Specifically, models using EQ included 148 to 182 frugivorous species. Other models included more reduced sample sizes (in species number): Striatum (56 to 63), MOB (34 to 39), Neocortex (61 to 69), Hippocampus (56 to 63), Cerebellum (62 to 70). Nonetheless, for a given set of models (i.e. within brain area), the sample was strictly identical, allowing within set comparison. Prior fitting, trait parameters were log-transformed to reach more symmetrical distributions. Models without competition, Brownian Motion (i.e. BM), Orstein-Uhlenbeck process (i.e. OU, model with stabilizing selection), or Early-Burst model (i.e. EB, for assessing a time-dependence of the evolutionary rate) were fitted using the “fitContinuous” function from the *geiger* package^{84,85}. Using the evolutionary history of species distribution (see [Primate species sympatry](#)) and of diet (see [Dietary guild](#)), we fitted competitive models using the “fit_t_comp” function from the *RPANDA* package⁸⁶. These competitive models notably account for interaction matrices that are built on the evolutionary history of species sympatry and diet. These interaction matrices retrace, along the phylogenetic tree, which frugivorous lineages were present within the same geographic areas (see Drury *et al.* [36]). We fitted three different competitive models. The matching competition model (MC) may consider divergence of traits of co-occurring lineages from a same dietary guild due to repulsion of traits (character displacement)³⁶. Here, that would mean that co-occurring species would tend to have either lower or higher EQ or relative brain size. Otherwise, we modelled trait evolution accounting for linear (DD_{lin}) or exponential (DD_{exp}) density-dependence^{36,87}. Density-dependence means that the evolutionary rate λ varies either positively or negatively as a function f of the number of co-occurring lineages sharing the same diet such as

$$\begin{aligned} f_{lin}(\lambda) &= \lambda_0 + rl \\ f_{exp}(\lambda) &= \lambda_0 \exp(rl) \end{aligned}$$

where λ_0 corresponds to the value of the initial ancestor, l indicates the number of lineages, r allows for modelling the speed and direction of the dependency to lineage number ($r > 0$ leads to an increase of trait changes, while $r < 0$ leads to a decline of the trait changes). All these models were repeated 10 times, using 10 different combination of the evolutionary history of ranging and diet. They were then compared within an information-theoretic framework³⁹ based on the weight of Akaike Information Criterion corrected for small samples (AICc) when considering all six models (MC, DD_{lin} , DD_{exp} , BM, OU, EB). The model weight then depicts the probability that it best describes the observed evolutionary pattern among the tested models.

(b) Dealing with data uncertainty and parameter sensitivity

In this analysis, uncertainty can stem from two sources. First, the true phylogeny is never known with certainty, and is estimated through Bayesian inference, thus we used the consensus tree from the 10kTrees project, which averages the phylogeny among 1000 possible estimated trees, given that running the models on several trees was too computationally demanding.

Similarly, the estimated evolutionary history of the diet and ranging might vary as well.

Second, for each species, trait estimates could vary slightly among datasets (see Appendix Figure S2). Particularly, although correlations seem good enough, it existed a variation in absolute measurement (Appendix Figure S2), while, in order to increase the overall number of species, trait values were not mandatorily from a single dataset. In addition, this study is based on several arbitrary thresholds, namely (i) to assess species sympatry (see Appendix Figure S1) and (ii) to assess the species dietary guild (see Appendix Figure S2) which can cause sensitivity of the results to the chosen parameters. To account for these three sources of variability we refitted several times the six models of trait evolution (BM, OU, EB, MC, DD_{lin} and DD_{exp}) with (1) random samples of the dietary and brain traits in case of multiple values available (i.e. equal probability for each possible value to be selected), (2) used the low or high threshold for assessing frugivory, folivory and geographic sympatry, and (3) various biogeography and dietary evolutionary history reconstructions.

Eventually, it means that the results for each model represent the average of 10 (uncertainty on diet/ranging evolution) \times 10 (uncertainty in brain/diet rate data) \times 2 (geographic overlap threshold) \times 2 (frugivory threshold) \times 2 (folivory threshold) = 800 sub-models. We stopped computations when the calculation of the likelihood was excessively long (> 1 week). The final sample size thus was of 730 models.

Models of species diversification

We investigated how primates diversified over time. Lineage-specific diversification rates were estimated using an updated version of the *ClaDS* algorithm⁴² boosted for computational speed based on data augmentation techniques⁴³. Particularly, we used *ClaDS2*, the model with constant turnover (i.e. constant ratio between extinction and speciation rates). This Bayesian approach considers speciation rate heterogeneity by modeling small shifts in the rate at speciation events. In other words, the daughter lineage is assumed to inherit new speciation rates that is sampled from a log-normal distribution with an expected mean value $\log(\alpha\lambda)$ (where λ represents the parental speciation rate and α is a trend parameter), and a standard deviation σ . Three independent chains were run until their respective convergence was validated by a Gelman-Rubin diagnostic criterion⁸⁸. The analysis relied on the use of a consensus tree of primate phylogeny from Dos Reis *et al.* [89]. This latter provides a robust phylogenetic tree for 367 primate species (while the 10kTrees primate phylogeny has only 301 species).

Such analysis necessarily depends on a prior estimation of the sample representativeness, that is, the fraction of sampled taxa (present in the phylogenetic tree) among all possible existing ones. Estrada *et al.* [90] estimated that, given current knowledge, the primate clade should be composed of 504 species. This means that the current sampling fraction is around 73%. We thus parameterized the *ClaDS* algorithm with this value for the estimate sampling fraction. Yet, given that the extant number of primate species is subject to controversy, and because the estimated sampling fraction may affect diversification rate estimations, we replicated our analyses with a range of sampling fractions from 95% down to 60%. At the end of each run, we extracted the maximum of the *a posteriori* net diversification rate of each extant primate species, as well as the mean diversification rate (given all lineages) through time.

Phylogenetic regressions

(a) Determining the direction of the selection gradient shaped by interspecific competition

To determine the nature of the relationship between species sympatry and relative sizes of brain regions, we fitted Gaussian Pagel's lambda phylogenetic regressions (i.e. a derivative of the Brownian Motion model, for which the phylogenetic variance-covariance matrix has all coefficients but its diagonal multiplied by lambda) for each brain region individually and for frugivorous species only. We used the Pagel's lambda model so as to relax the hypothesis of Brownian Motion since we included brain areas for which the evolutionary history was best described by competitive models. Here specifically, we considered the least stringent frugivory assessment, with frugivory threshold fixed to 20%, folivory threshold fixed to 40%. If, due to data variability, a species did not robustly fit into the categorical classification "frugivorous versus folivorous" (i.e. could be either of the two), it was considered as frugivorous nonetheless.

The response variable was the relative size of brain areas shown as better described by competitive phylogenetic scenario (see above). Due to data variability, we took the mean of the possible values given the different datasets, and assessed the sensitivity using non-averaged values (see [Phylogenetic regressions: results, stability and assumption](#)). In this model, the covariates (i.e. continuous predictors) were the average percent of the range surface overlapping with other sympatric frugivorous species, and the number of frugivorous sympatric species (the second was square rooted, to reach symmetrical distribution). For a given species A, sympatry with another species B was considered when species B range overlapped on more than 10% of the range of species A. This was done to reduce noise induced by coarse identification of species range.

(b) Diversification and brain size

In the same way than explained above, we fitted Gaussian Pagel's lambda phylogenetic regressions of the different relative brain sizes against the diversification rate (i.e. accounting for both, speciation and extinction) estimated for each species by the *ClaDS* algorithm. Again, we took the mean of the brain trait values for the main model and assessed the sensitivity by re-running the model several times using non-averaged values in this case.

(c) Diversification and sympatry

To determine whether sympatry was associated to specific diversification pattern (and thus if diversification rates were regionalized), we fitted Gaussian Pagel's lambda phylogenetic regressions with the diversification rate as output variable, and used the two metrics for describing sympatry (the average percent of the range surface overlapping with other sympatric frugivorous species, and the number of frugivorous sympatric species) as tested variables, as described in (a).

(d) Model implementation

(i) Direction of the selection gradient shaped by interspecific competition

Models were fitted using the “*phylolm*” function from the *phylolm* package⁹¹, with the lambda parameter (i.e. indicating whether the trait is subject to selection, or corresponds to Brownian Motion, if λ tends towards 1) estimated by maximum-likelihood (argument “model” set to “lambda”). Bootstrapping over 1000 independent replicates was done so as to obtain confidence intervals. Other function parameters were set to default. Prior fitting, covariates were symmetrized if necessary. Necessary assumptions on the normal distribution of residuals and homoscedasticity were visually assessed and pointed out no violation (see Appendix [Model assumptions](#)). We did not observe correlation issue among predictors either ($VIF_{max} < 2$, Mundry [92]).

(ii) Diversification and brain size

We could not compute phylogenetic regressions to link diversification and brain traits in frugivorous primates using a frequentist approach because it led to violation of homoscedasticity. Instead, we fitted Bayesian phylogenetic regressions using the “*MCMCglmm*” function of the *MCMCglmm* package⁹³. Each chain was based on a burnin period of 5000 iterations, among a total of 5×10^4 iterations, and was sampled every 50 iterations. We used the least informative priors. Fixed priors were let to default (Gaussian distribution of mean 0 and variance 10^8). Prior on random effects and residuals were set to follow an inverse-Wishart distribution with a variance at limit (V) of 1, and a degree of belief (nu) of 0.02. We checked model convergence by fitting three chains, and calculated the Gelman-Rubin criterion (max value < 1 ; Gelman & Rubin [88]), as well as checked autocorrelation (max absolute value < 0.07) using the respective “gelman.diag” and “autocorr.diag” functions from the *coda* package⁹⁴. In Appendix [Model assumptions](#), we present trace and distributions of posterior estimates. We further checked the quality of the posterior by visually assessing the Q-Q plot of the posterior with that of a Gaussian distribution of mean 0 and sd 1 (see Appendix [Model assumptions](#)). We present the estimate together with the 95% credibility interval centered on the mode (Highest Density Posterior, HDP), together with a MCMC p-value (pMCMC) that corresponds to the probability that the estimate (β) is positive if the mean estimate ($\hat{\beta}$) is negative (i.e. $P(\beta > 0 | \hat{\beta} < 0)$), or if the mean estimate is positive, the probability that the estimate is negative (i.e. $P(\beta < 0 | \hat{\beta} > 0)$).

(iii) Diversification and sympatry

We fitted phylogenetic regression as explained in (i). In particular, verification of model assumption and stability pointed out no source of worry (see [Phylogenetic regressions: results, stability and assumption](#)).

(d) Model robustness

To assess frequentist model stability with regards to singular points, we computed the DfBetas (variation in estimates) by discarding one observation at a time of the “standard” dataset used to fit the main model, based on the consensus tree.

To assess the sensitivity to (i) the variability in data and (ii) phylogeny uncertainty, we

refitted the models using 50 phylogenetic trees among the 10000 possible trees from the 10kTrees project. For each of these trees, we fitted the model 50 times, allowing random sampling for data when we had multiple values (e.g. if body mass was provided by different datasets etc.). For the diversification analysis specifically, we also assessed the sensitivity to changes in primate sampling fraction by refitting the models for values ranging between 60 to 95% (as specified before) using the “standard” dataset and the consensus tree.

The results of these assessment (min-max of estimates) are shown in Appendix [Model stability](#). It emphasizes weak sensitivity of the results.

Acknowledgements

We considerably value the help provided by Jonathan Drury in making some scripts available, but mostly for helping us in solving issues encountered with the use of functions of his own in the *RPANDA* package in *R*, and that of Marie-Claude Quidoz for assistance for using the CEFÉ cluster. We thank Simon Benhamou and Manon Clairbaux for discussion and advices on spatial projections, and M. Quérroué, V. Lauret, A. Caizergues and C. Teplisky for feedback on Bayesian computations too. Finally, this work could not have been possible without prior data collection from the IUCN Red List (primate ranging), the 10kTrees project (phylogenetic trees), and Alexandra R. DeCasien and collaborators, Lauren E. Powell and collaborators, Orlin S. Todorov and collaborators, Erik P. Willems and collaborators, Fiona Pearce and collaborators, Navarrete and collaborators, and Cyril C. Grueter who provided primate trait data we used as (supplementary) material with their articles, as well as Nicholas J. Matzke for available algorithm scripts allowing us to implement and better understand the methods. Their indirect input is therefore tremendous. Both authors were supported by a doctoral grant from the *École Normale Supérieure*, Paris.

Authors’ contribution

BR conceived the study, collected, cleaned and analyzed the data, drew the figures and wrote the first version of the manuscript and subsequently revised it. BP-L implemented the ClaDS algorithm for our data, helped with running other analyses, and revised the manuscript multiple times. The authors declare having no conflict of interest. All authors gave final approval for publication and agree to be held accountable for the work performed therein.

Table 1: Model estimates and significance of phylogenetic regressions to assess the selection gradient direction | Est.=Estimate, CI2.5%=Lower border of the CI95%, CI97.5%=Upper border of the CI95%, Sd=Standard deviation, t=Statistics t-value. The brain area (as well as the associated sample size) are indicated prior each list of estimates. The transformation applied to variables are indicated between brackets (logarithm, log, or square-root, sqrt), as well as the ponderation by bodymass (/bodymass).

	Est.	CI2.5%	CI97.5%	Sd	t	p-value
EQ (log) (N=127)						
Intercept	-0.17	-0.53	0.22	0.20	-	-
% of overlapped home range	0.02	-0.08	0.13	0.05	0.41	0.68
Number of sympatric frugivorous (sqrt)	0.02	-0.02	0.05	0.02	1.03	0.31
Lambda	0.98	0.94	1.00			
Hippocampus (/bodymass, log) (N=50)						
Intercept	-0.92	-1.95	0.05	0.53	-	-
% of overlapped home range	-0.39	-0.76	-0.01	0.20	-1.94	0.06
Number of sympatric frugivorous (sqrt)	0.08	-0.06	0.20	0.07	1.21	0.23
Lambda	0.99	0.92	1.00			
Neocortex (/bodymass, log) (N=56)						
Intercept	2.07	1.31	2.86	0.41	-	-
% of overlapped home range	-0.23	-0.54	0.11	0.16	-1.46	0.15
Number of sympatric frugivorous (sqrt)	0.02	-0.08	0.13	0.05	0.48	0.63
Lambda	0.99	0.91	1.00			
Cerebellum (/bodymass, log) (N=57)						
Intercept	0.60	-0.15	1.35	0.39	-	-
% of overlapped home range	-0.08	-0.32	0.17	0.12	-0.7	0.49
Number of sympatric frugivorous (sqrt)	-0.01	-0.1	0.07	0.04	-0.34	0.74
Lambda	1.00	0.96	1.00			
Striatum (/bodymass, log) (N=50)						
Intercept	-0.36	-1.18	0.44	0.44	-	-
% of overlapped home range	-0.40	-0.77	-0.04	0.18	-2.26	0.03
Number of sympatric frugivorous (sqrt)	0.03	-0.08	0.15	0.06	0.61	0.54
Lambda	0.98	0.85	1.00			
MOB (/bodymass, log) (N=31)						
Intercept	-2.76	-4.61	-0.93	1.00	-	-
% of overlapped home range	-1.20	-2.65	0.35	0.80	-1.49	0.15
Number of sympatric frugivorous (sqrt)	0.21	-0.18	0.56	0.19	1.12	0.27
Lambda	1.00	1e-07	1.00			

Table 2: Model estimates and significance of Bayesian phylogenetic regressions to assess the correlation between diversification and brain size | Est.=Estimate, HDP2.5%=Lower border of the 95% Highest Posterior Density, HDP97.5%=Upper border of the 95% Highest Posterior Density, Eff. samp.=Effective sample (adjusted for autocorrelation). The brain area (as well as the associated sample size) are indicated prior each list of estimates. The logarithm transformation was applied to variable and is indicated between brackets (log), as well as the ponderation by bodymass (/bodymass).

	Est.	HDP2.5%	HDP97.5%	Eff. samp	pMCMC
Diversification EQ (N=148)					
Intercept	0.12	0.08	0.16	900.00	-
EQ (log)	0.02	-7.91e-03	0.05	789.25	0.15
Lambda	0.83	0.76	0.9		
Diversification Hippocampus (N=61)					
Intercept	0.13	0.09	0.18	900.00	-
Hippocampus (/bodymass, log)	9.10e-03	-9.48e-03	0.03	900.00	0.34
Lambda	0.73	0.6	0.85		
Diversification Neocortex (N=67)					
Intercept	0.1	0.04	0.17	991.53	-
Neocortex (/bodymass, log)	7.26e-03	-0.02	0.03	900.00	0.56
Lambda	0.74	0.6	0.86		
Diversification Cerebellum (N=68)					
Intercept	0.12	0.07	0.16	900.00	-
Cerebellum (/bodymass, log)	3.94e-03	-0.02	0.03	989.21	0.76
Lambda	0.74	0.6	0.86		
Diversification Striatum (N=61)					
Intercept	0.12	0.08	0.17	900.00	-
Striatum (/bodymass, log)	9.11e-03	-0.01	0.03	900.00	0.44
Lambda	0.73	0.59	0.85		
Diversification MOB (N=37)					
Intercept	0.11	0.05	0.17	900.00	-
MOB (/bodymass, log)	-4.79e-03	-0.02	0.01	900.00	0.59
Lambda	0.65	0.46	0.83		

Table 3: Model estimates and significance of phylogenetic regressions to assess the correlation between diversification and sympatry | Est.=Estimate, CI2.5are indicate prior each list of estimates. the transformation (logarithm or square-root) if indicated in parenthese by the abbreviation (log or sqrt).

	Est.	CI2.5%	CI97.5%	Sd	t	p-value
Diversification (N=128)						
Intercept	0.15	0.10	0.2	0.03	-	-
% of overlapped home range	-5.40e-03	-0.02	9.35e-03	8.14e-03	-0.66	0.51
Number of sympatric frugivorous (sqrt)	-5.04e-03	-0.01	1.34e-04	2.56e-03	-1.97	0.05
Lambda	0.96	0.89	0.99			

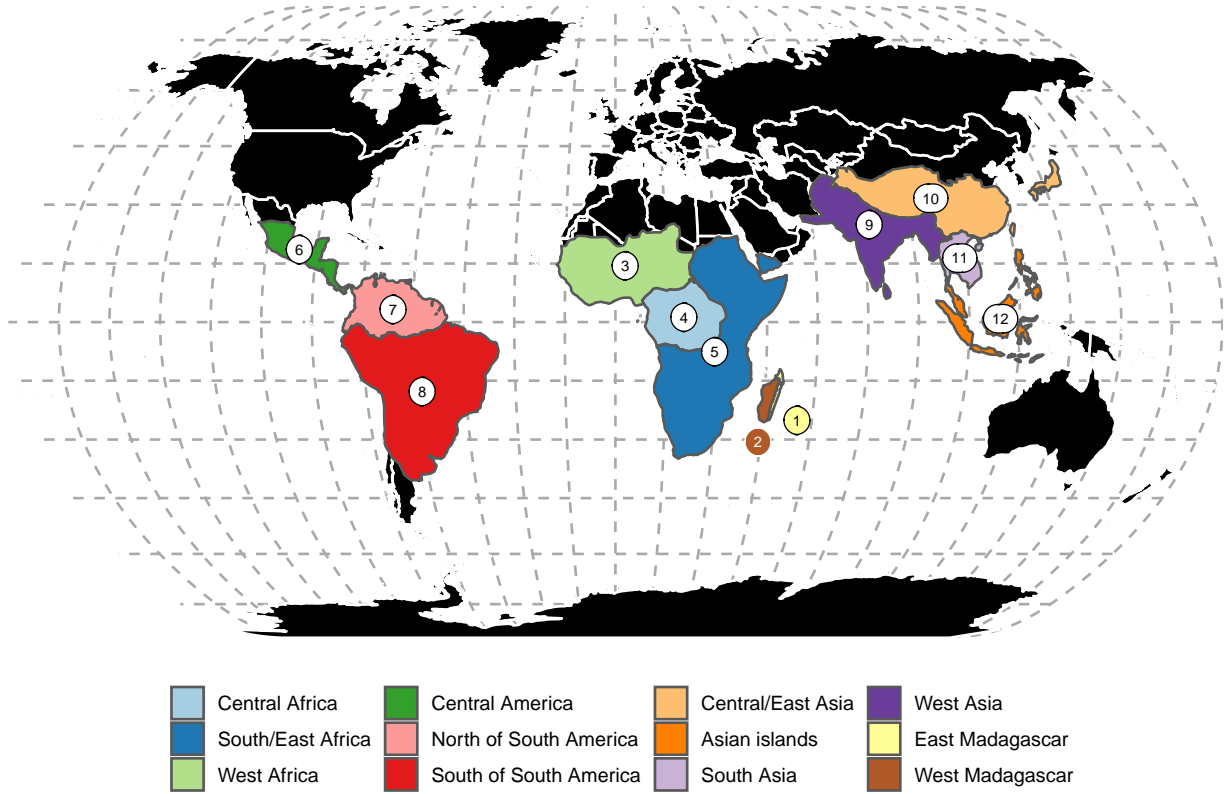


Figure 1: Geographic areas used for ancestral range reconstruction represented on the Natural Earth projection of the world | Areas were defined as a combination of geographic and environmental criteria relatively to the primate taxonomy following results from³³: (1) East Madagascar (2) West Madagascar (3) West Africa (4) Central Africa (5) East/South Africa (6) Central America (7) North South-America (8) South South-America (9) West Asia (10) Central/East Asia (11) South Asia (12) Asian peninsula and islands. Note that the north part of Africa and the south of Europe were discarded despite the presence of one primate species (*Macaca sylvanus*), because of its geographical complete isolation and repeated intervention of human people in population maintenance⁹⁵. Hence, *Macaca Sylvanus* is not considered in this study.

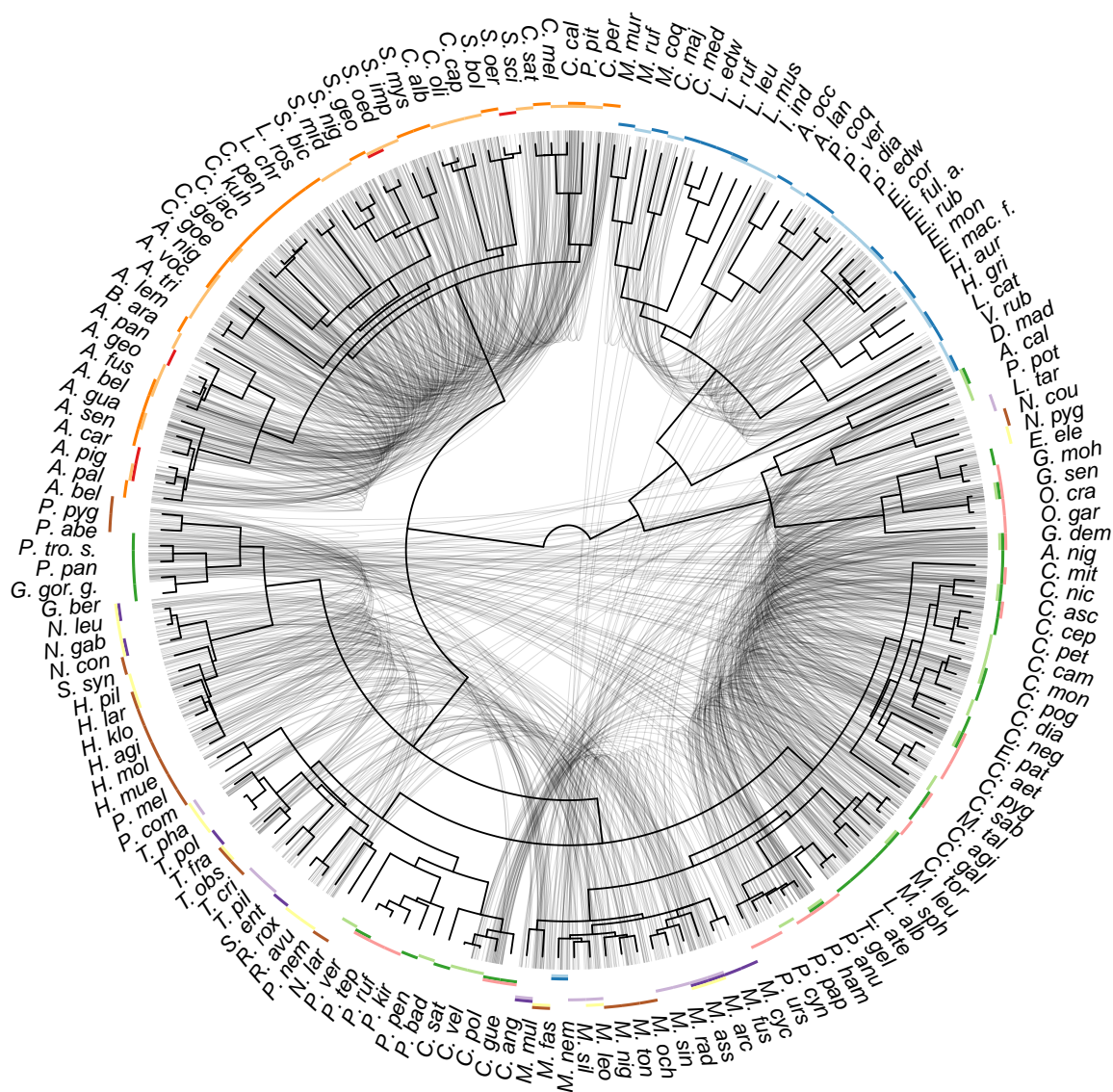


Figure 2: Current frugivorous primate sympatry pattern and phylogeny | Primate phylogeny from a consensus tree of 1000 possible trees from the 10kTrees project is depicted in the centre, together with abbreviated species name. The corresponding non-abbreviated names can be found using Appendix Figure S3. Co-occurring frugivorous (based on a frugivory threshold of 20% and folivory of 40%) species are linked by lightgray lines. The geographic area occupied by a species is depicted by the coloured rectangles. Presence was assed given an overlap between the species range and the geographic area of 10%.

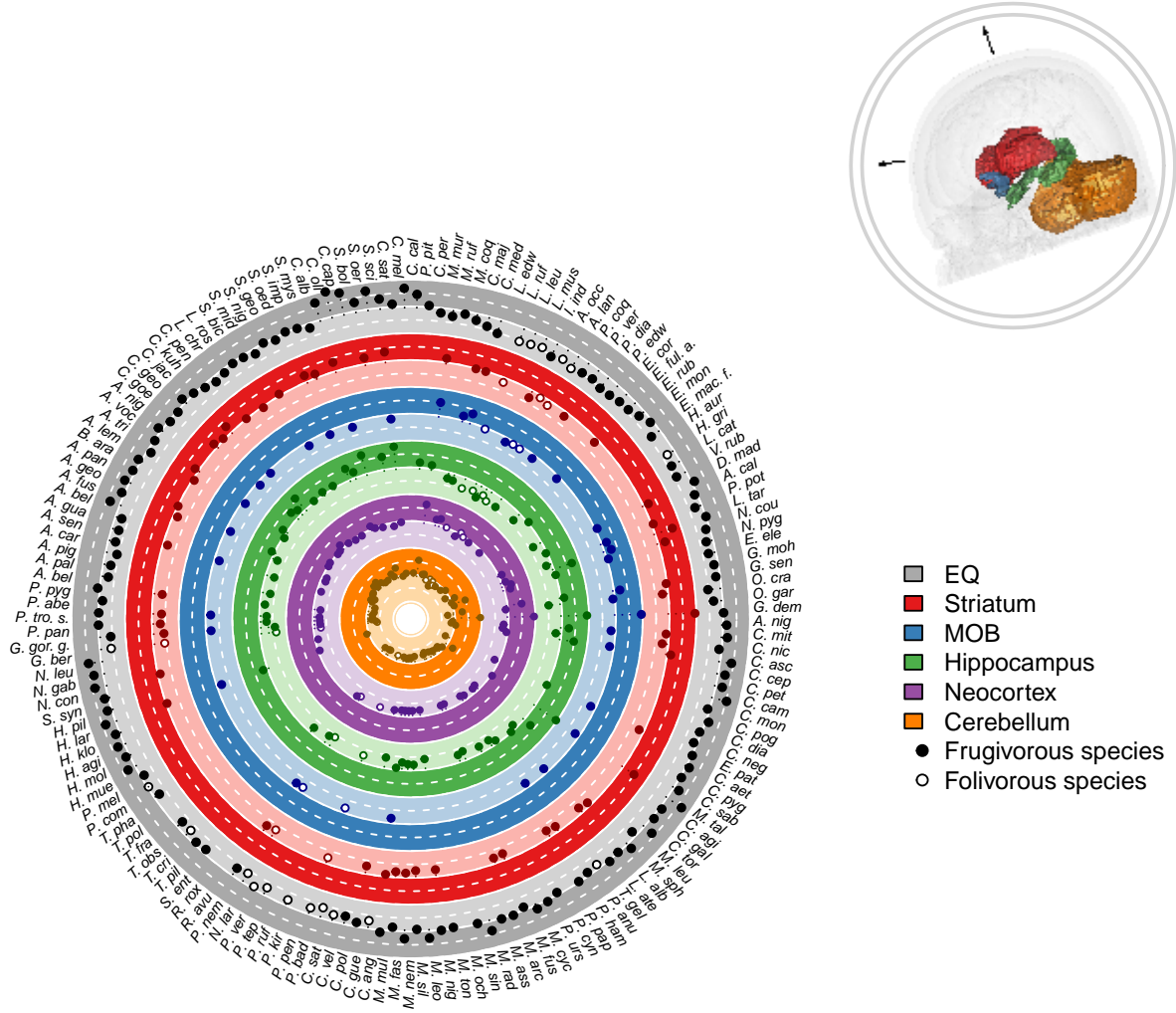


Figure 3: (Left) EQ or relative brain size value among frugivorous primates (Right) Studied brain areas | (Left) The circular rows are indicated by the colours which match a specific brain area. The darker background emphasises when values are above average, while the lighter background emphasises when values are below average. The mean value (after scaling and based on one random sampling among possible values, but see S2 for visualization of measure variability) for the Encephalization Quotient (EQ) or relative size of brain parts, when available, is depicted by a plain circle for frugivorous species. The frugivorous threshold was fixed to 20% and folivory to 40%. (Right) A 3D brain from *Homo sapiens* is depicted (*neurobase* package⁹⁶, *misc3d* package⁹⁷). The arrows indicate the sagittal and frontal axes. Studied brain area are coloured, although the neocortex was not coloured for readability since it corresponds to the external layer of the cerebral hemisphere. In short, the MOB is involved in immediate olfactory information processing, the Neocortex and the Cerebellum support a working memory and memory consolidation processes^{24–26}, and the Hippocampus supports a working memory and a long-term spatio-temporal memory²¹. The Striatum is involved in social information processing¹⁸.

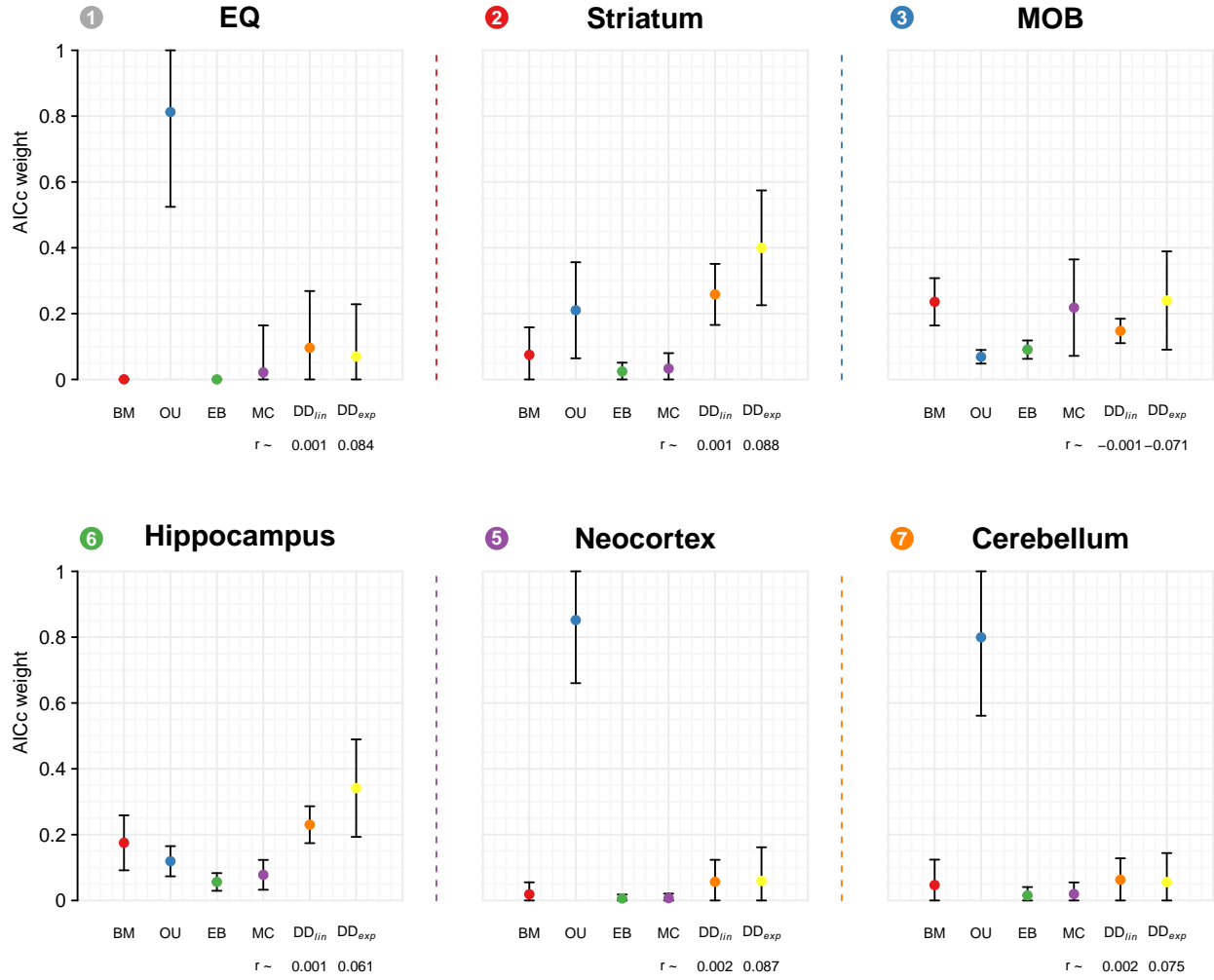


Figure 4: Relative support of fitted models of trait evolution for each brain part | Plotted is the AICc weight, a measure of relative support for a given model, for non-competitive (BM, OU, EB) and competitive (MC, DD_{lin} , DD_{exp}) models. The points represent the average AICc weight obtained (when considering the six models from a same run), while the vertical bars indicate the standard deviation given all tested conditions (see [Models of trait evolution: does interspecific interactions shape brain size evolution?](#)).

Appendix

Data availability

Availability of trait and distribution range for the 301 primate species represented in the primate phylogeny of the 10kTrees project is depicted in Appendix Figure S3.

Data variability

We present below the results of the assessments of data variability depending on the considered thresholds (for frugivory, folivory or overlap) and the data set that is used, specifically related to distribution ranges, or anatomical/behavioural traits.

Sensitivity to variation in distribution range

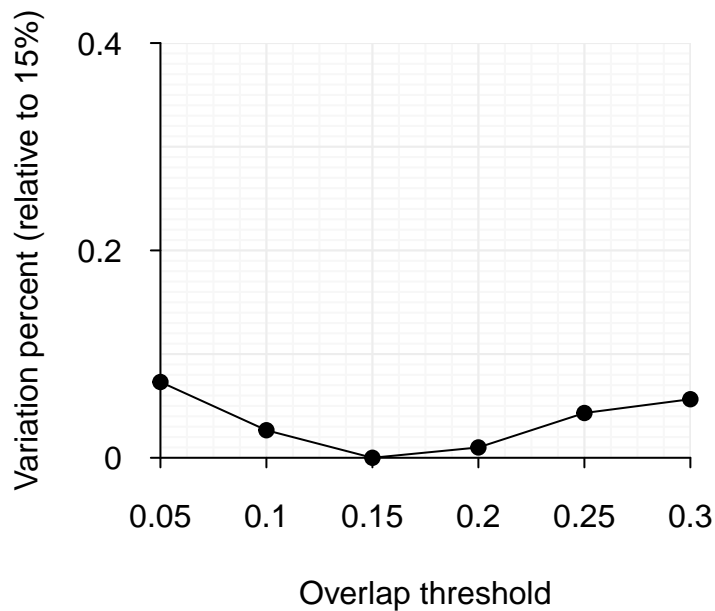


Figure S1: Percent of species with differently identified biogeographic areas in function of the overlap threshold (reference is an overlap threshold of 15%) | For a given species, a biogeographic area difference means that at least one biogeographic area considers absence/presence of the species while this was not the case with the 15% threshold. 15% was chosen as the reference since halfway to the chosen maximum of 30%. 30% was chosen as the maximum because based on current observations, a species occupied at best three different biogeographic areas.

Sensitivity to variation in trait value

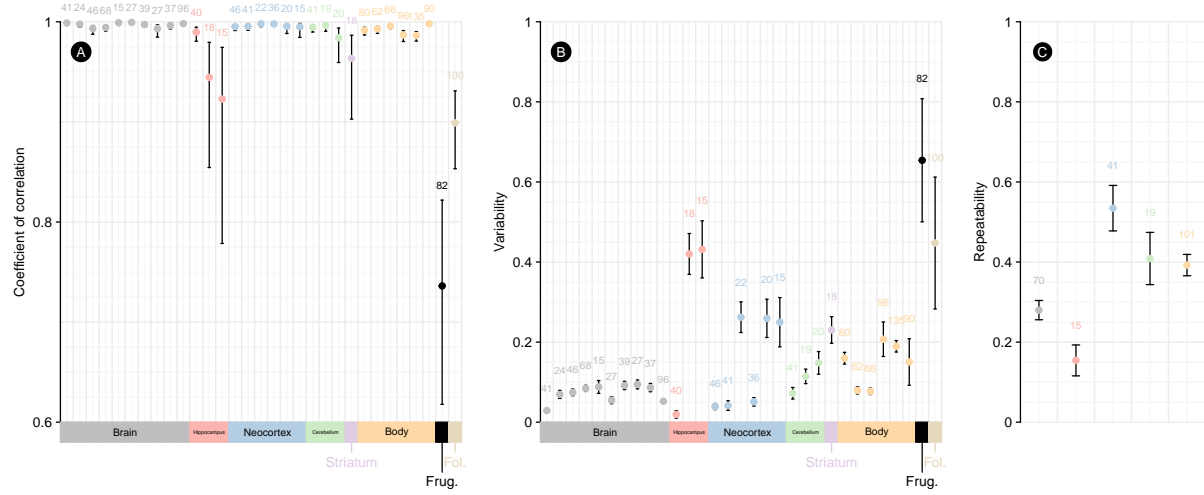


Figure S2: Supplementary Figure. Variation in trait values among reference datasets | Colours are associated to a specific trait: Brain, Hippocampus, Neocortex and Cerebellum refers to the volume of the area (in mm^3), Body refers to the body mass (in g), Frug. indicates the frugivory rate and Fol. indicates the folivory rate. (A) Correlation: The points depict the coefficient of correlation while the bar depicts the 95% confidence interval (CI). (B) Variability: The points depict the average of the mean ratio m of the absolute of differences with paired values; If we reduce the equation, we have $m = |(v_1^2 - v_2^2)| / (2v_1v_2)$, where v_1 and v_2 are the two paired values from two different datasets and are different from 0. If v_1 and v_2 equal 0, then $m = 0$. If v_1 or v_2 equals 0 (case for the diet rates constrained between $[0,1]$), then we fixed the null value to 0.01. The bar depicts the standard error. (C) Repeatability: Repeatability was assessed for traits that were included in at least three datasets. Prior calculation, traits were pondered *within* species by the *within* species max value. The point represents the mean repeatability r calculated as $\sigma_{between}^2 / (\sigma_{between}^2 + \sigma_{within}^2)$, with the $\sigma_{between}^2$ and σ_{within}^2 corresponding the variance *between* or *within* species. The bar depicts the standard error. For all graphics, sample sizes are indicated above the upper value of the CI/error interval.

Primate diversification rate over time

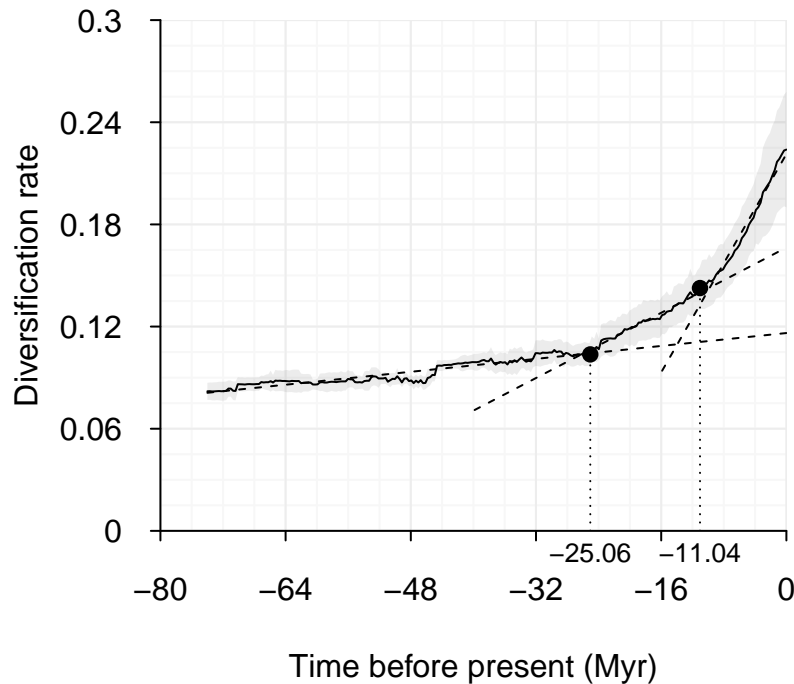


Figure S4: Diversification rate over time in the Primate taxon | The average diversification rate estimated based on an assumed sampling fraction of primate species ranging from 60 to 90% (at a step of 10%) is depicted by the plain line. The grey background depicts the standard deviation. The two breakpoints, depicted by the plain dots and the vertical dotted bars, were thus estimated based on a three-linear regression segmentation using the *strucchange* package [Zeileis *et al.* [98]; Zeileis *et al.* [99]; Zeileis [100]; see the vignette package for statistical details]. The three fitted regressions are displayed by the dashed lines. The choice of two breakpoints was priorly assessed by choosing the number of breakpoints minimizing the the Bayesian Information Criterion. The identified breakpoints coin with identified sharp decrease in extinction rate^{101,102} due to the emergence of more favourable environmental conditions stemming from a progressive warming after harsh temperature cooling that started earlier in the Oligocene until reaching a mid-Miocene Climatic Optimum¹⁰³.

Phylogenetic regressions: results, stability and assumption

Model results

- (a) Phylogenetic regressions: selection gradient

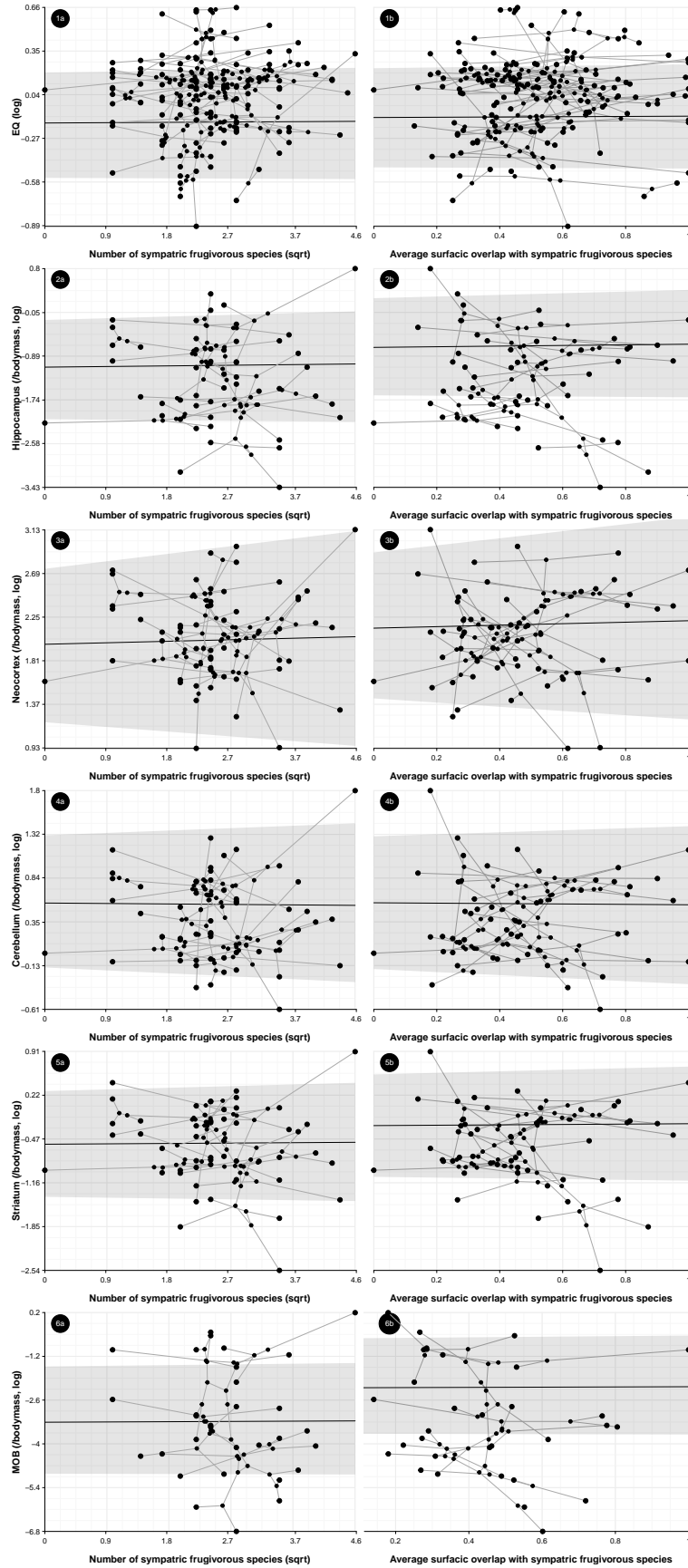


Figure S5: Phylogenetic regressions of relative brain size in function of sympatry intensity indices | Left graphics depict the effect of the number of sympatric species on the brain size, when the effect of the percentage of the distribution range overlapped by sympatric species is averaged, while the right graphics do the opposite. Raw data are depicted with points, while the segments that link them correspond to the projected phylogenetic tree. The model fit is shown with the plain black line and the associated 95% confidence interval is depicted by the transparent gray background.

(b) Phylogenetic regressions: diversification and brain size

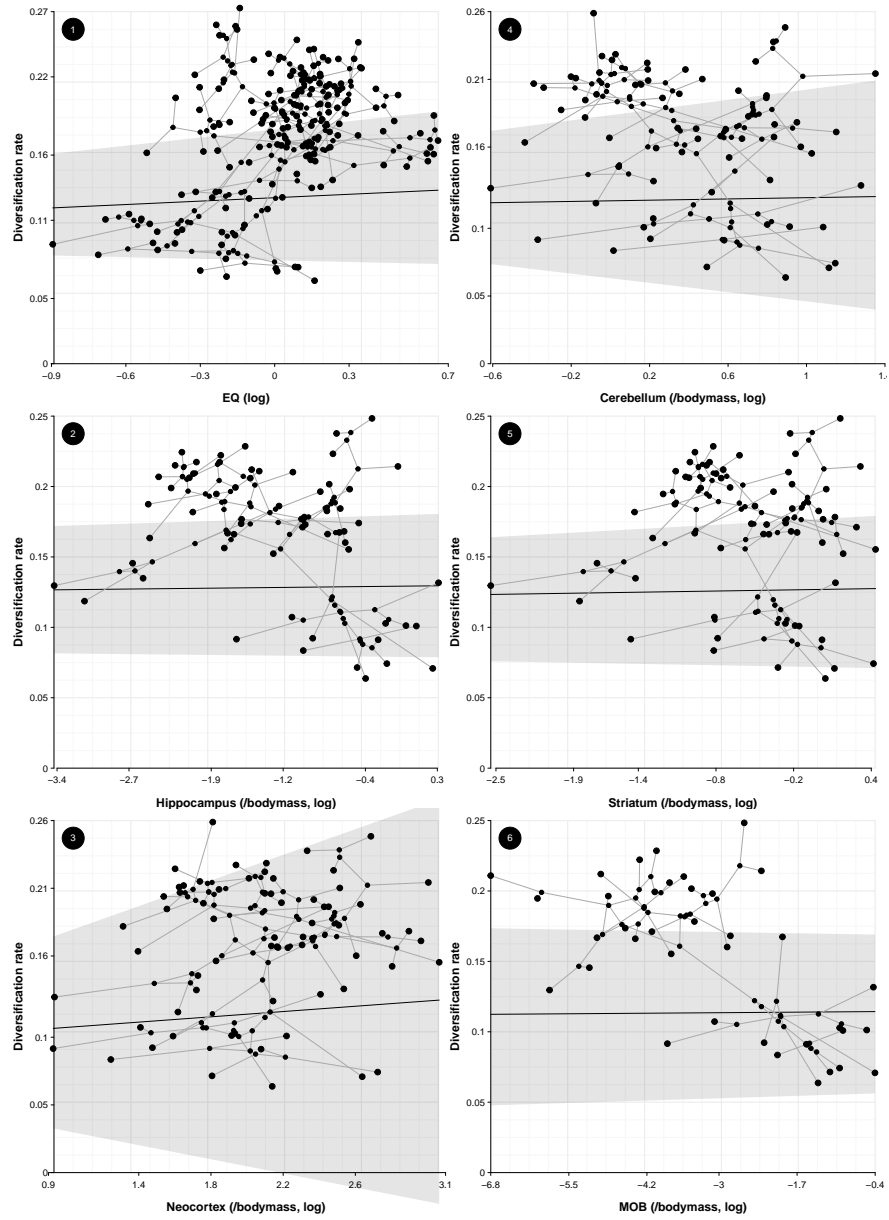


Figure S6: Phylogenetic regressions of the diversification rate in function of the size of the different brain areas | Raw data are depicted with points, while the segments that link them correspond to the projected phylogenetic tree. The model fit is shown with the plain black line and the associated 95% highest density posterior is depicted by the transparent gray background.

(b) Phylogenetic regressions: diversification and sympatry

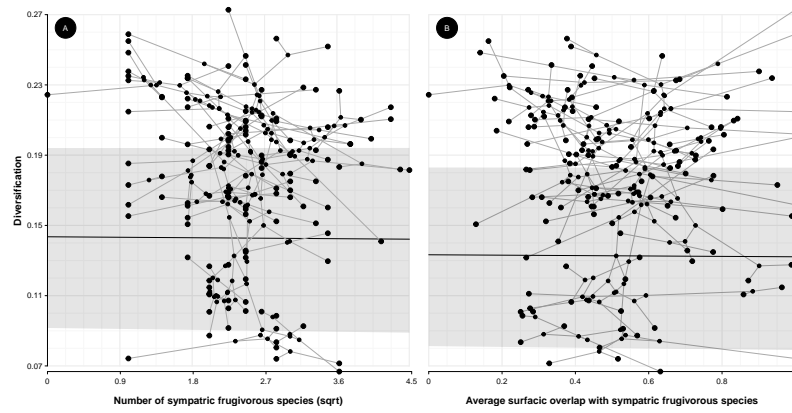


Figure S7: Phylogenetic regressions of diversification rate in function of sympatry intensity indices | Left graphics depict the effect of the number of sympatric species on the brain size, when the effect of the percentage of the distribution range overlapped by sympatric species is averaged, while the right graphics do the opposite. Raw data are depicted with points, while the segments that link them correspond to the projected phylogenetic tree. The model fit is shown with the plain black line and the associated 95% confidence interval is depicted by the transparent gray background.

(d) Forest plot of estimates

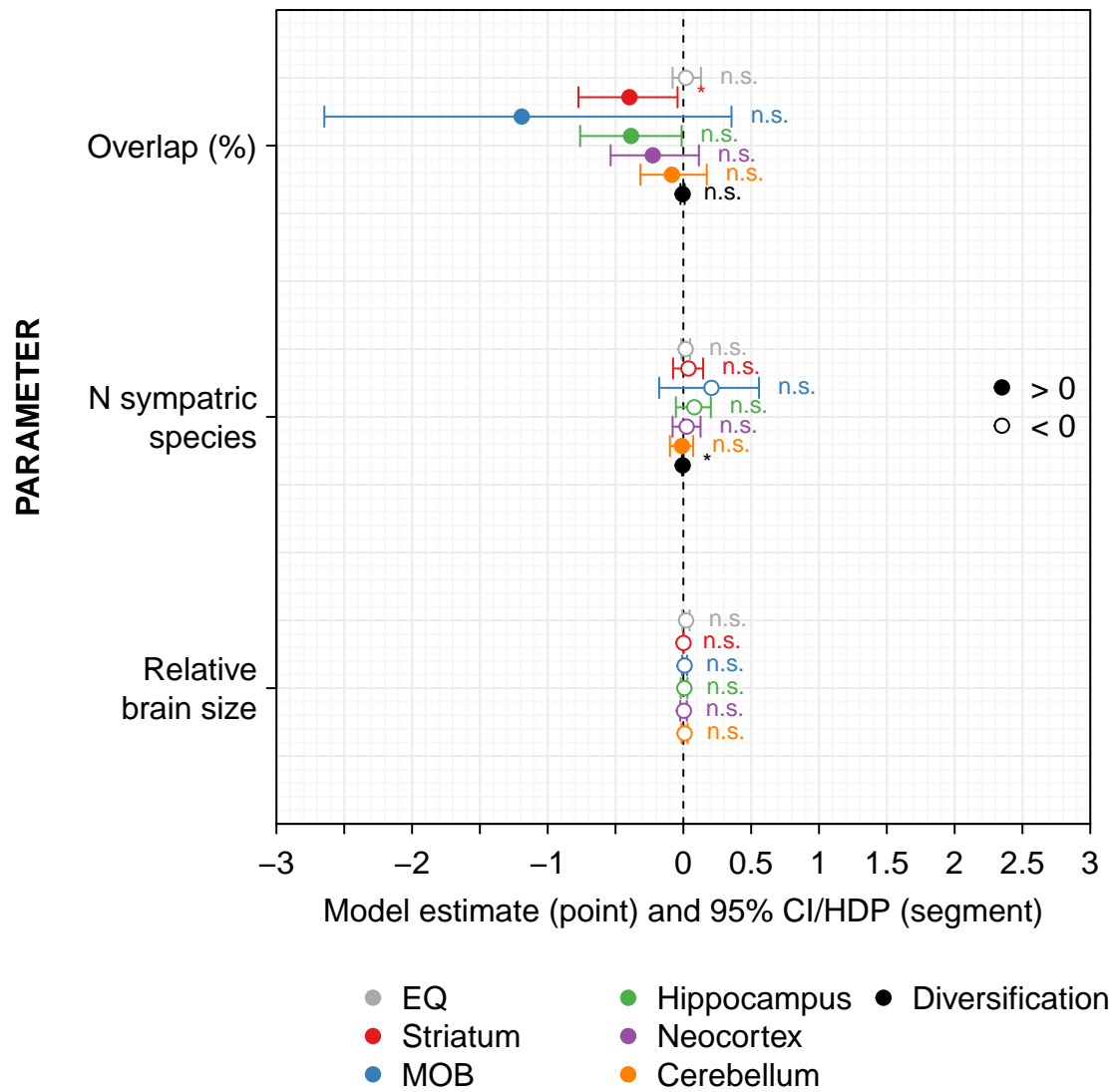


Figure S8: Forest plot of the phylogenetic regressions | CI: Confidence Interval, HDP: Highest Posterior Density (when brain size is the predictor, they are barely visible because reduced). Plain dots depict negative effects, open dots depict positive effects.

Model stability

We present below statistical indicators related to changes in estimates when re-fitting the model considering sub-samples (i.e. DfBetas and Cook's distance), as well as when accounting for data variability (i.e. re-sampling among possible values given all datasets) or when using different parameterisation (i.e. "sampling fraction" of known species for diversification analysis).

(a) Phylogenetic regressions: selection gradient

Table S1: Sensitivity analysis of phylogenetic regressions to assess the relationship between speies sympatry and relative brain sizes | Depicted is the minimum and maximum of estimates when one observation was removed at a time (DfBetas) or when varying the used phylogenetic tree and the data sampling (Phylogeny/Data).

Regression		DfBetas			Phylogeny/Data		
Trait	Variable	Est. min.	Est.	Est. max.	Est. min.	Est.	Est. max.
Cerebellum (/bodymass, log)	Intercept	0.55	0.6	0.67	0.22	0.6	0.7
	Overlap	-0.16	-0.08	-0.03	-0.49	-0.08	-4.84e-03
	N co-occurrence	-0.04	-0.01	5.27e-03	-0.01	-0.01	0.17
	Lambda	1	1	1	0.3	1	1
EQ (log)	Intercept	-0.19	-0.17	-0.13	-0.41	-0.17	-0.05
	Overlap	7.14e-04	0.02	0.06	-0.38	0.02	0.09
	N co-occurrence	5.37e-03	0.02	0.02	2.70e-03	0.02	0.1
	Lambda	0.98	0.98	0.99	0.35	0.98	1
Hippocampus (/bodymass, log)	Intercept	-1.03	-0.92	-0.82	-1.16	-0.92	-0.41
	Overlap	-0.5	-0.39	-0.2	-1.37	-0.39	-0.28
	N co-occurrence	0.04	0.08	0.1	0.03	0.08	0.21
	Lambda	0.99	0.99	1	0.79	0.99	1
MOB (/bodymass, log)	Intercept	-3.23	-2.76	-2.62	-2.99	-2.76	-2.55
	Overlap	-1.83	-1.2	-0.8	-1.5	-1.2	-0.87
	N co-occurrence	0.11	0.21	0.33	0.13	0.21	0.26
	Lambda	1	1	1	1	1	1
Neocortex (/bodymass, log)	Intercept	1.95	2.07	2.23	1.73	2.07	2.32
	Overlap	-0.31	-0.23	-0.03	-0.55	-0.23	-0.02
	N co-occurrence	-0.02	0.02	0.06	-0.04	0.02	0.15
	Lambda	0.98	0.99	1	0.23	0.99	1
Striatum (/bodymass, log)	Intercept	-0.45	-0.36	-0.26	-0.76	-0.36	-0.07
	Overlap	-0.46	-0.4	-0.28	-0.92	-0.4	-0.22
	N co-occurrence	4.03e-03	0.03	0.06	0.01	0.03	0.18
	Lambda	0.98	0.98	1	0.79	0.98	1

(b) Phylogenetic regressions: diversification and brain size

Table S2: Sensitivity analysis of phylogenetic regressions to detect the assess the relationship between species diversifition and relative brain sizes| Depicted is the minimum and maximum of estimates when varying the used phylogenetic tree and the data sampling (Phylogeny/Data), or when the sampling fraction varied (Sampling fraction).

Regression		Phylogeny/Data			Sampling fraction		
Model	Variable	Est. min.	Est.	Est. max.	Est. min..1	Est..1	Est. max..1
Cerebellum (/bodymass, log)	Intercept	0.12	0.12	0.12	0.11	0.12	0.13
	Trait	7.60e-04	3.94e-03	4.17e-03	1.91e-04	3.94e-03	6.13e-03
	Lambda	0.69	0.74	0.74	0.72	0.74	0.75
EQ (log)	Intercept	0.12	0.12	0.12	0.11	0.12	0.13
	Trait	7.51e-03	0.02	0.02	6.04e-03	0.02	0.02
	Lambda	0.77	0.83	0.83	0.8	0.83	0.85
Hippocampus (/bodymass, log)	Intercept	0.13	0.13	0.13	0.12	0.13	0.14
	Trait	3.73e-03	9.10e-03	9.10e-03	4.07e-03	9.10e-03	9.10e-03
	Lambda	0.69	0.73	0.73	0.72	0.73	0.75
MOB (/bodymass, log)	Intercept	0.1	0.11	0.11	0.1	0.11	0.12
	Trait	-9.89e-03	-4.79e-03	-4.76e-03	-7.64e-03	-4.79e-03	-4.10e-03
	Lambda	0.6	0.65	0.65	0.64	0.65	0.65
Neocortex (/bodymass, log)	Intercept	0.1	0.1	0.11	0.1	0.1	0.12
	Trait	4.69e-03	7.26e-03	7.26e-03	1.60e-03	7.26e-03	7.26e-03
	Lambda	0.69	0.74	0.74	0.72	0.74	0.75
Striatum (/bodymass, log)	Intercept	0.12	0.12	0.13	0.12	0.12	0.14
	Trait	5.89e-03	9.11e-03	9.41e-03	6.27e-03	9.11e-03	9.13e-03
	Lambda	0.69	0.73	0.73	0.72	0.73	0.75

Table S3: Sensitivity analysis of phylogenetic regressions to assess the selection diversificationAndSympatry direction | Depicted is the minimum and maximum of estimates when one observation was removed at a time (DfBetas) or when varying the used phylogenetic tree and the data sampling (Phylogeny/Data)

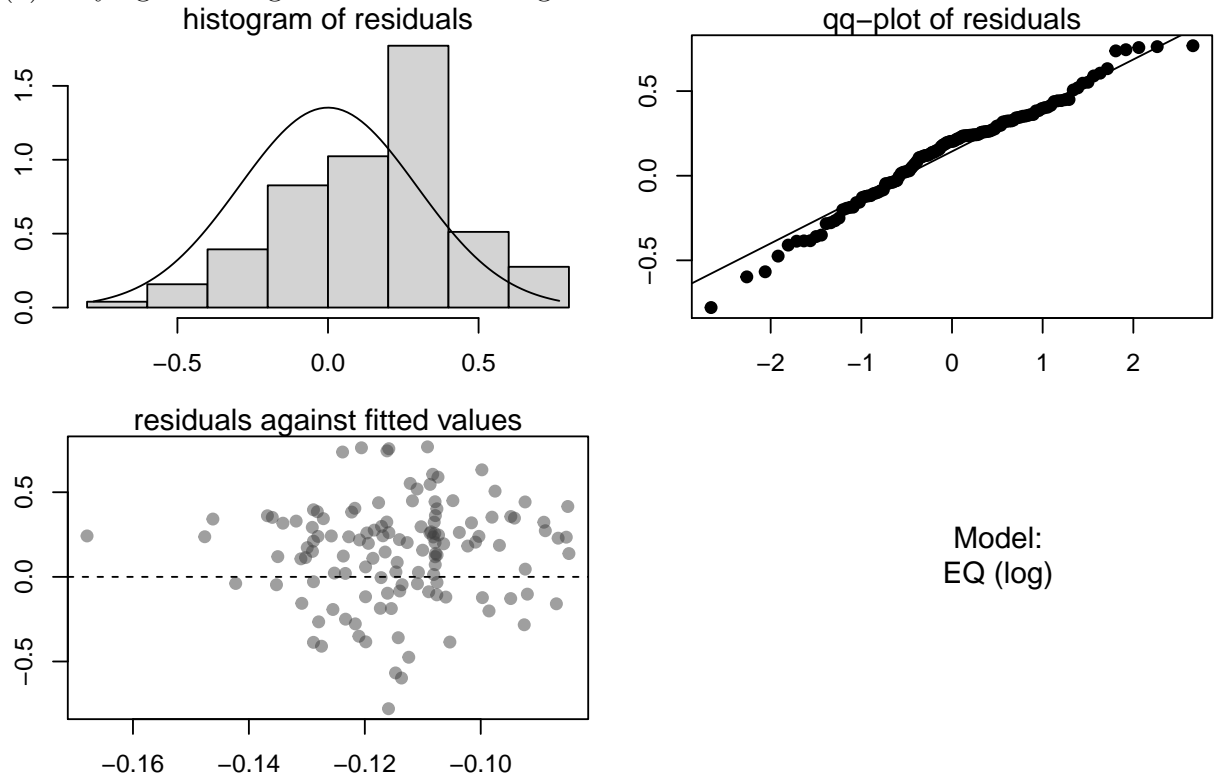
Model:		DfBetas			Phylogeny/Data			Sampling fraction	
Variable	Est. min.	Est.	Est. max.	Est. min.	Est.	Est. max.	Est. min.	Est.	Est. max.
Intercept	0.14	0.15	0.15	0.15	0.15	0.15	0.14	0.15	0.17
Overlap	-8.58e-03	-5.40e-03	5.85e-05	-5.73e-03	-5.40e-03	-5.73e-03	-8.6e-03	-5.40e-03	7.71e-03
N co-occurrence	-6.03e-03	-5.04e-03	-4.24e-03	-5.2e-03	-5.04e-03	-5.2e-03	-9.06e-03	-5.04e-03	-6.14e-03
Lambda	0.96	0.96	0.97	0.96	0.96	0.96	0.94	0.96	0.99

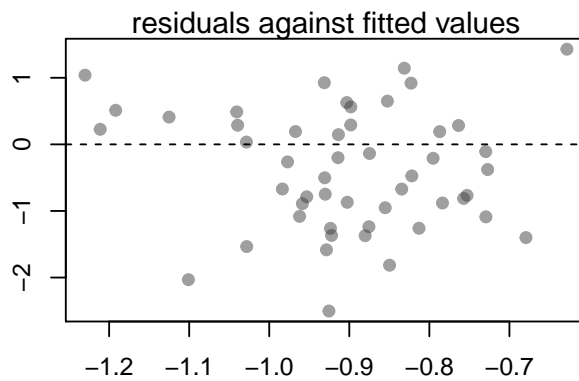
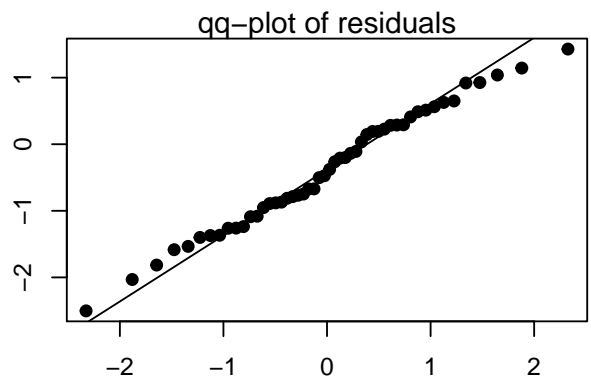
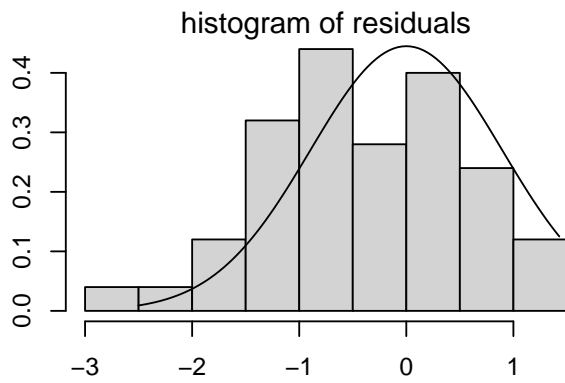
(b) Phylogenetic regressions: diversification and sympatry

Model assumptions

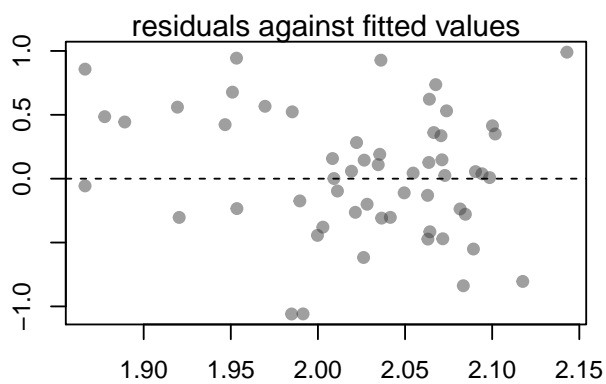
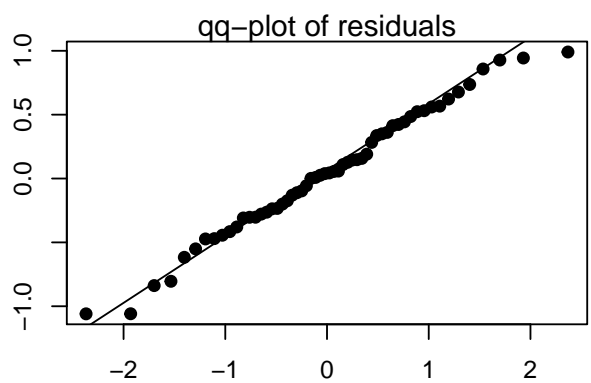
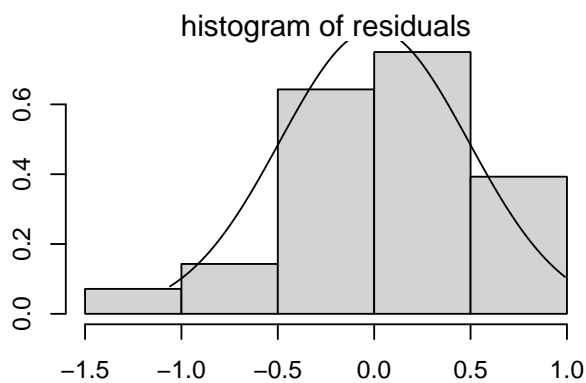
We present below the visual assessment of linear modelling assumptions (histogram of residuals, Q-Q plot, and scatterplot of fitted values vs residuals).

(a) Phylogenetic regressions: selection gradient

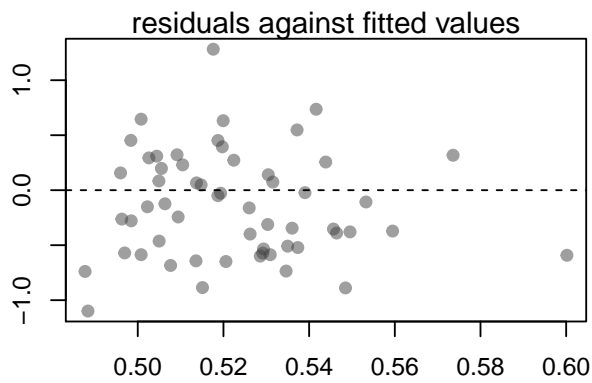
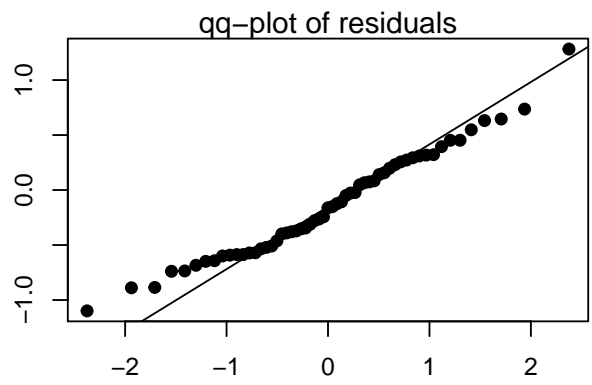
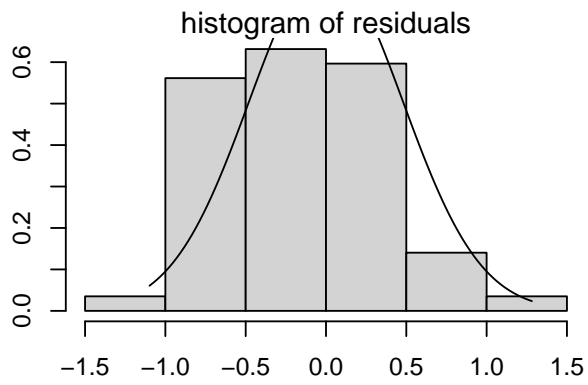




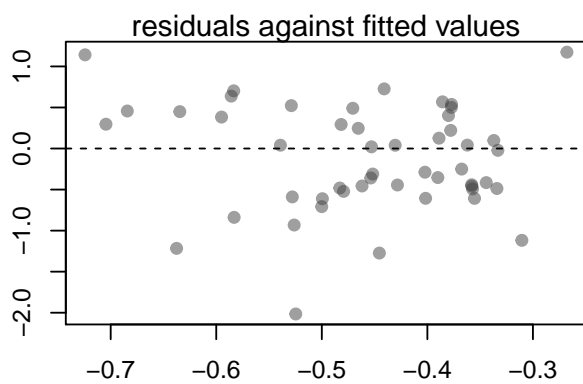
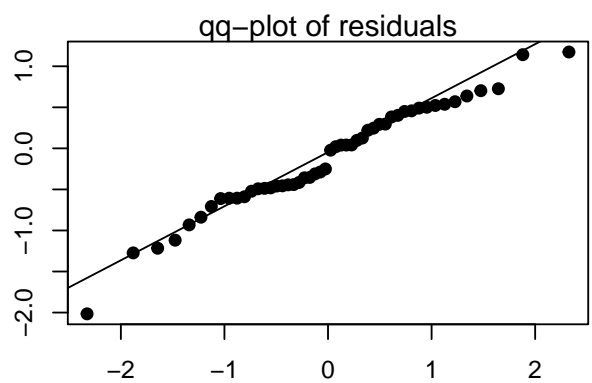
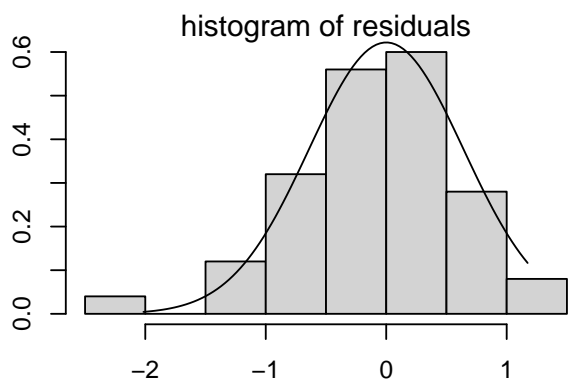
Model:
Hippocampus (/bodymass, log)



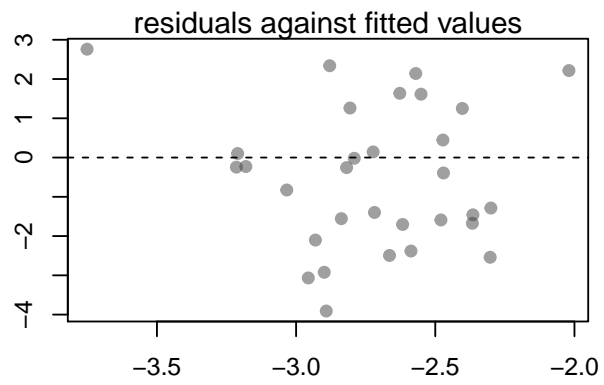
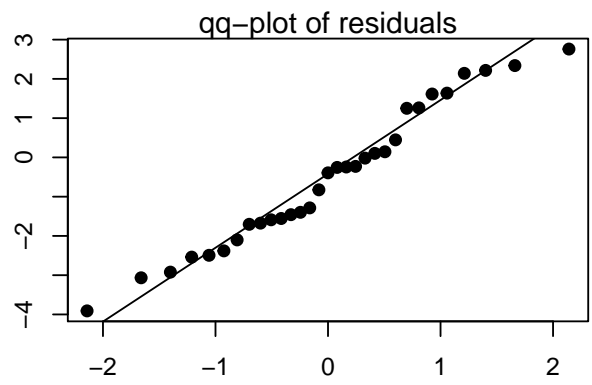
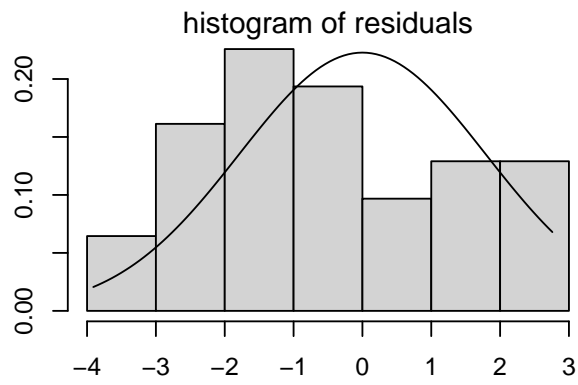
Model:
Neocortex (/bodymass, log)



Model:
Cerebellum (/bodymass, log)



Model:
Striatum (/bodymass, log)

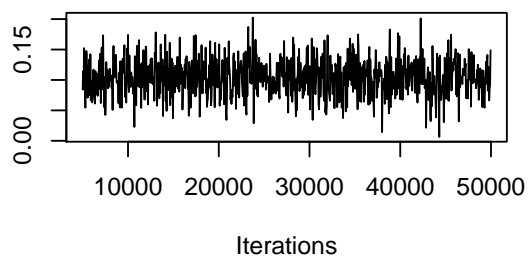


Model:
MOB (/bodymass, log)

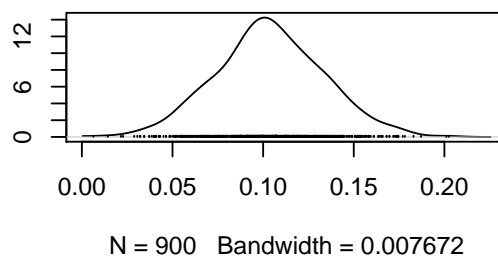
(b) Phylogenetic regressions: diversification and brain size

Fixed effects: EQ (log)

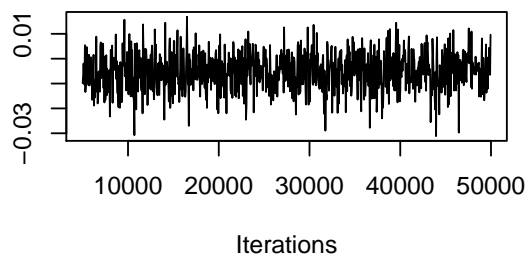
Trace of (Intercept)



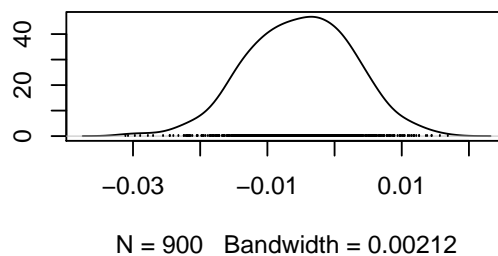
Density of (Intercept)



Trace of Trait

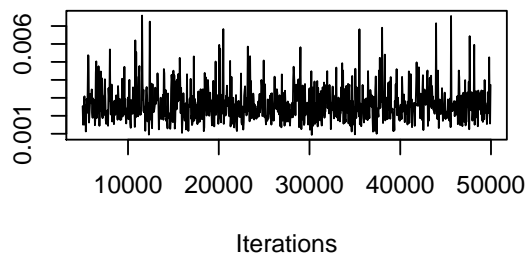


Density of Trait

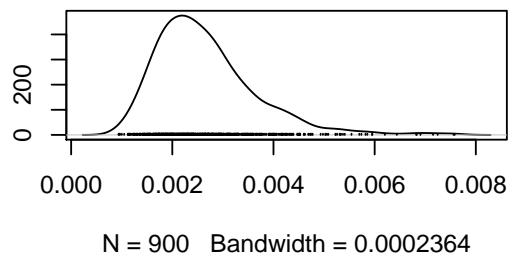


Random/residuals: EQ (log)

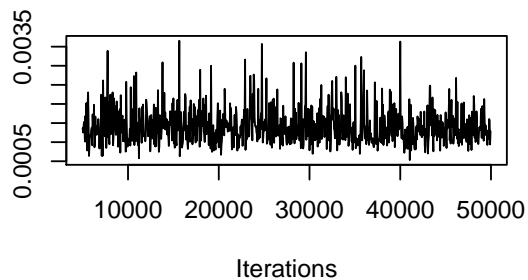
Trace of Species



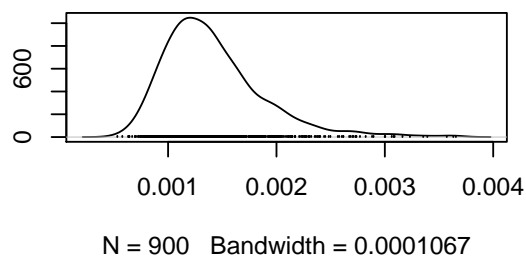
Density of Species



Trace of units

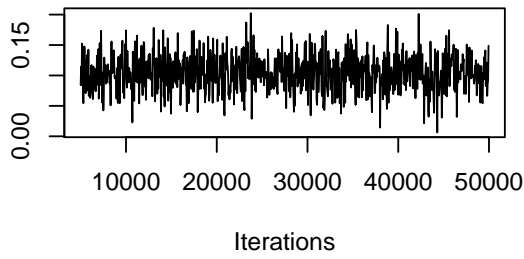


Density of units

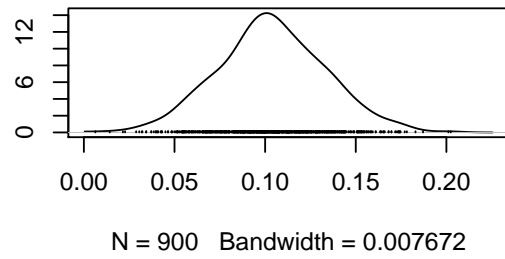


Fixed effects: Hippocampus (/bodymass, log)

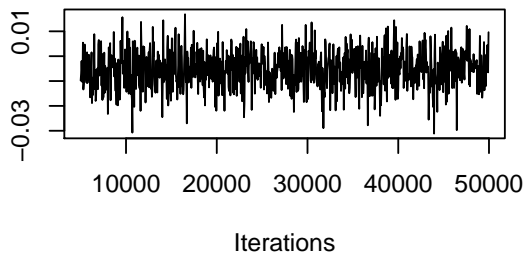
Trace of (Intercept)



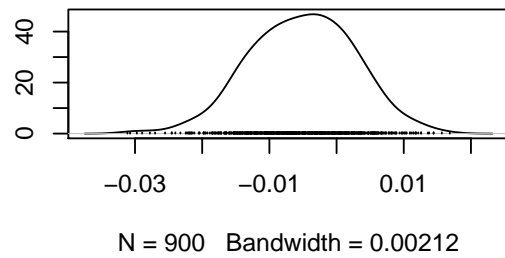
Density of (Intercept)



Trace of Trait

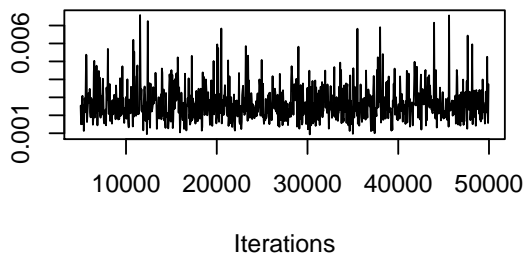


Density of Trait

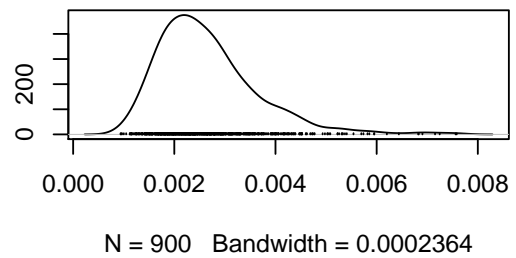


Random/residuals: Hippocampus (/bodymass, log)

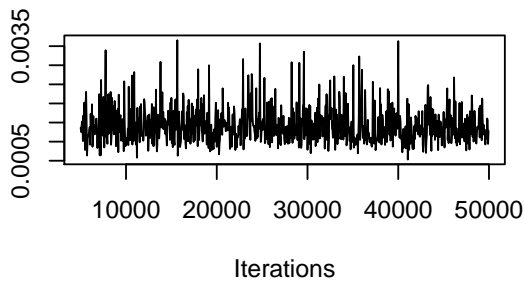
Trace of Species



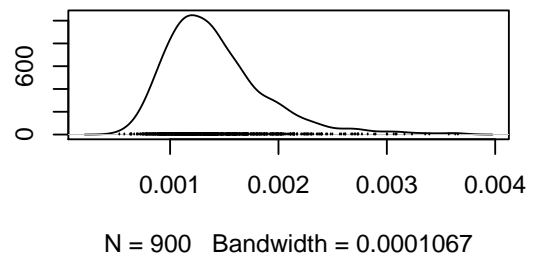
Density of Species



Trace of units

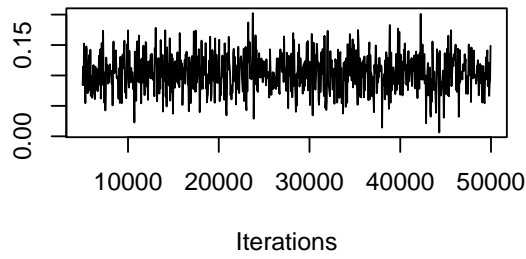


Density of units

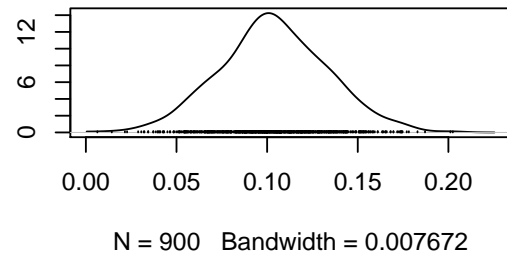


Fixed effects: Neocortex (/bodymass, log)

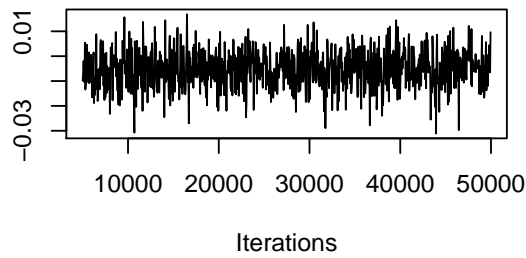
Trace of (Intercept)



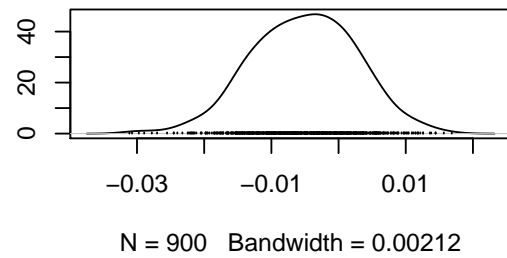
Density of (Intercept)



Trace of Trait

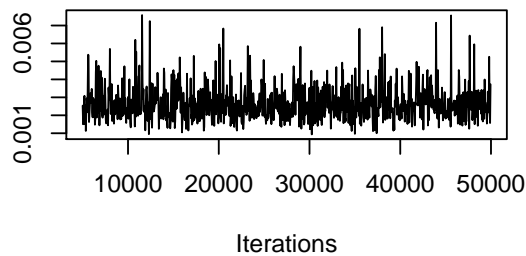


Density of Trait

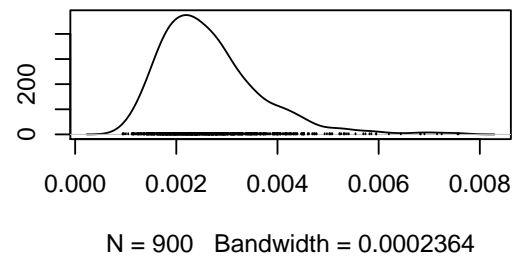


Random/residuals: Neocortex (/bodymass, log)

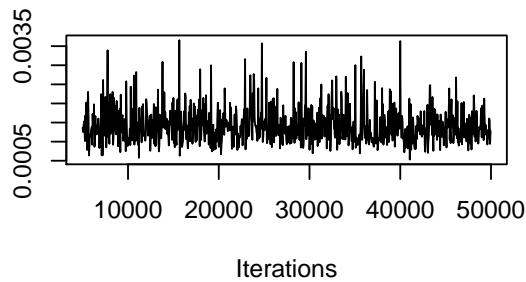
Trace of Species



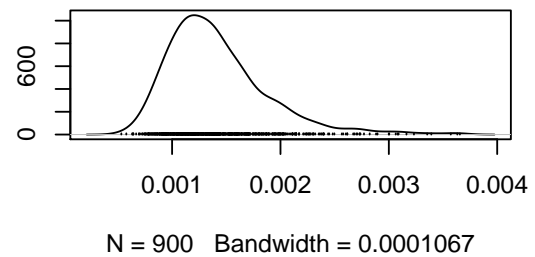
Density of Species



Trace of units

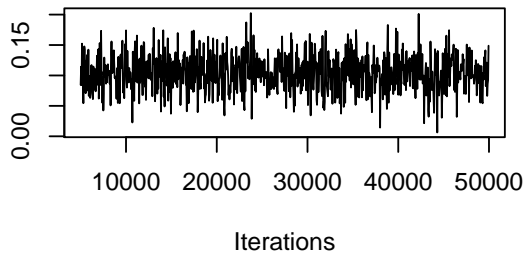


Density of units

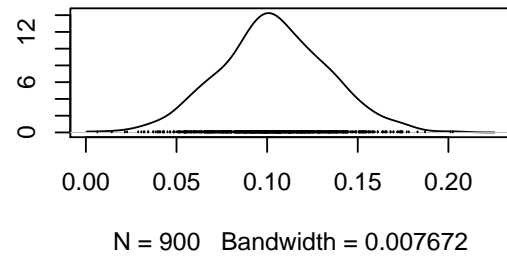


Fixed effects: Cerebellum (/bodymass, log)

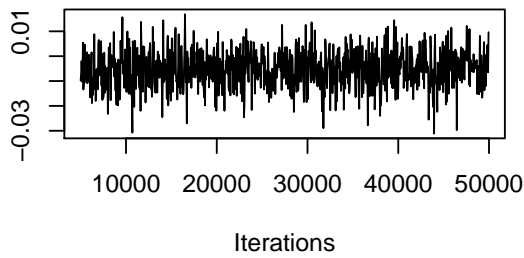
Trace of (Intercept)



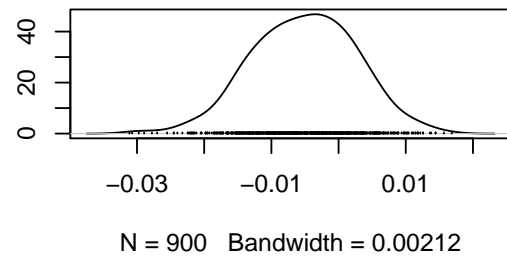
Density of (Intercept)



Trace of Trait

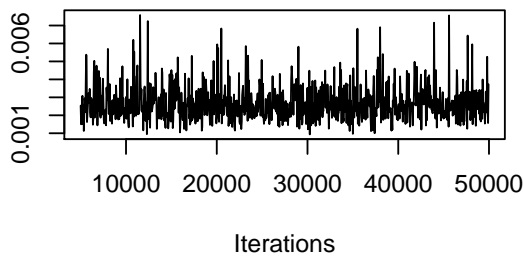


Density of Trait

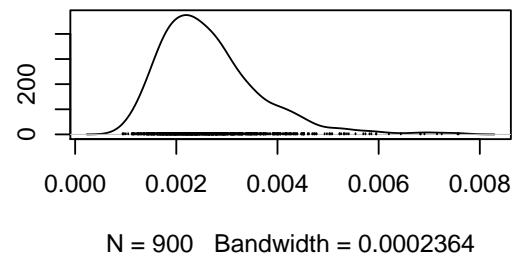


Random/residuals: Cerebellum (/bodymass, log)

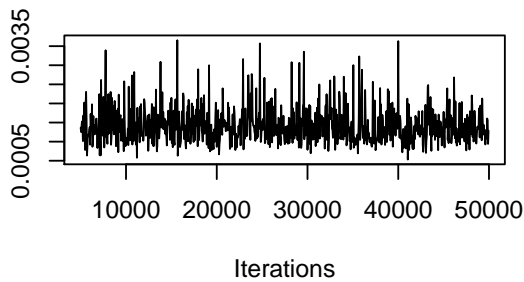
Trace of Species



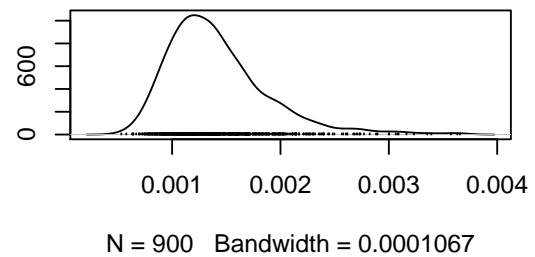
Density of Species



Trace of units

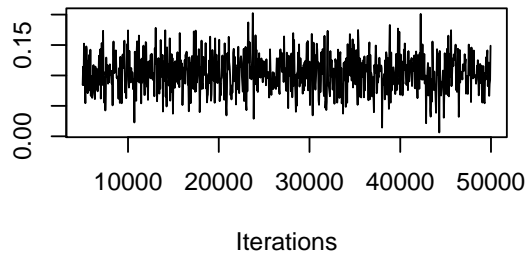


Density of units

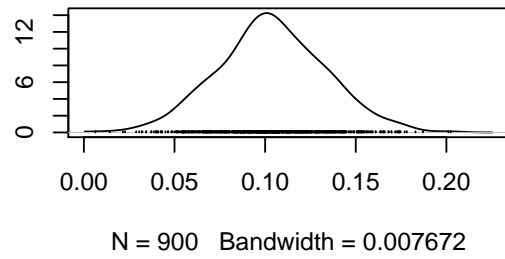


Fixed effects: Striatum (/bodymass, log)

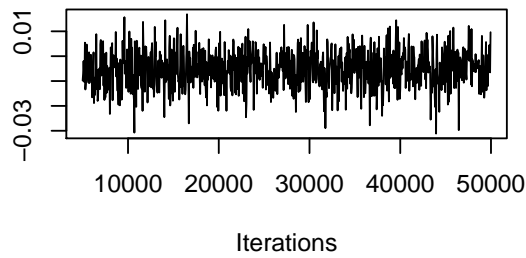
Trace of (Intercept)



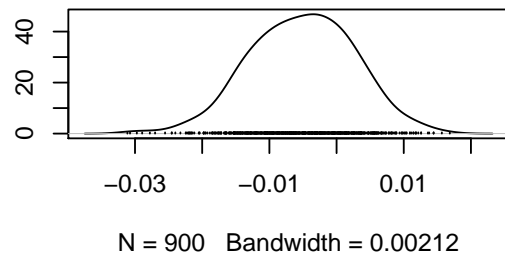
Density of (Intercept)



Trace of Trait

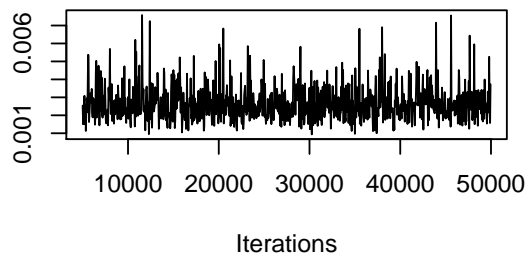


Density of Trait

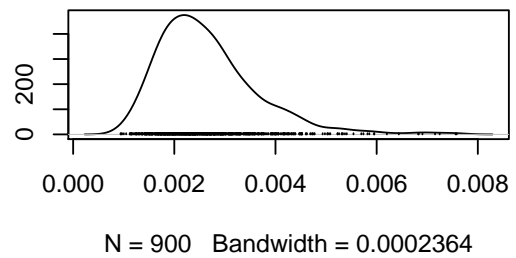


Random/residuals: Striatum (/bodymass, log)

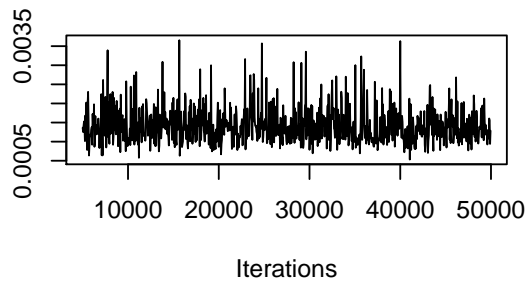
Trace of Species



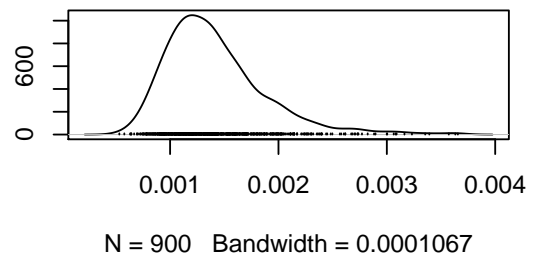
Density of Species



Trace of units

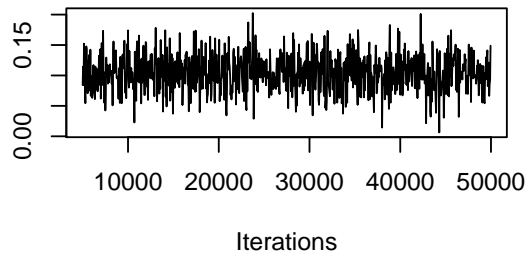


Density of units

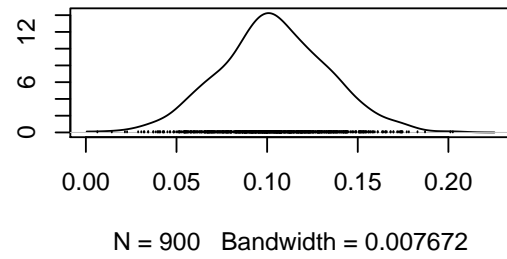


Fixed effects: MOB (/bodymass, log)

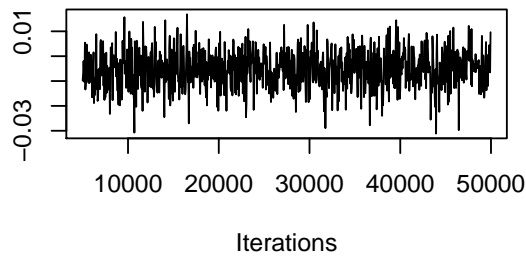
Trace of (Intercept)



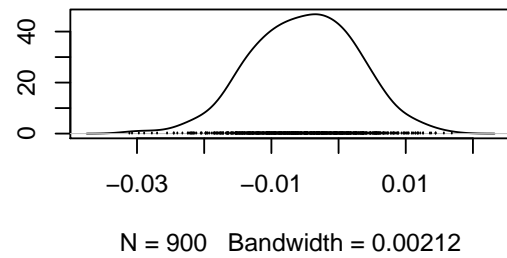
Density of (Intercept)



Trace of Trait

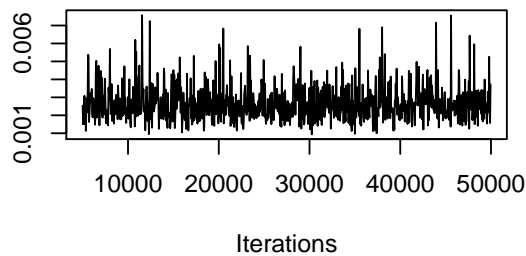


Density of Trait

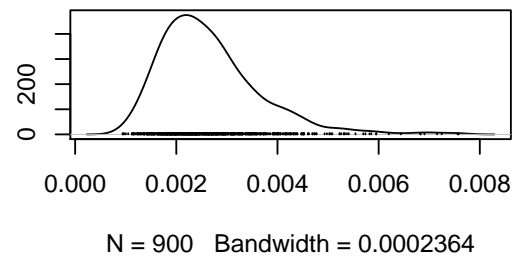


Random/residuals: MOB (/bodymass, log)

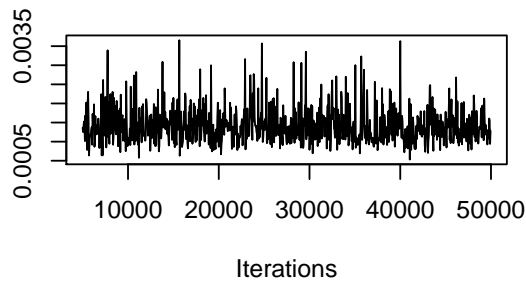
Trace of Species



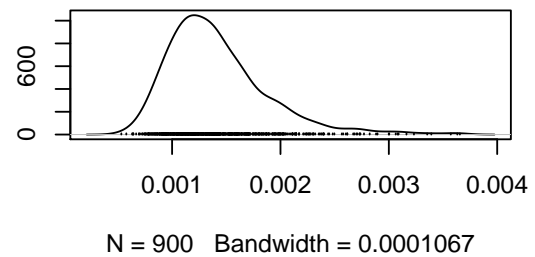
Density of Species



Trace of units



Density of units



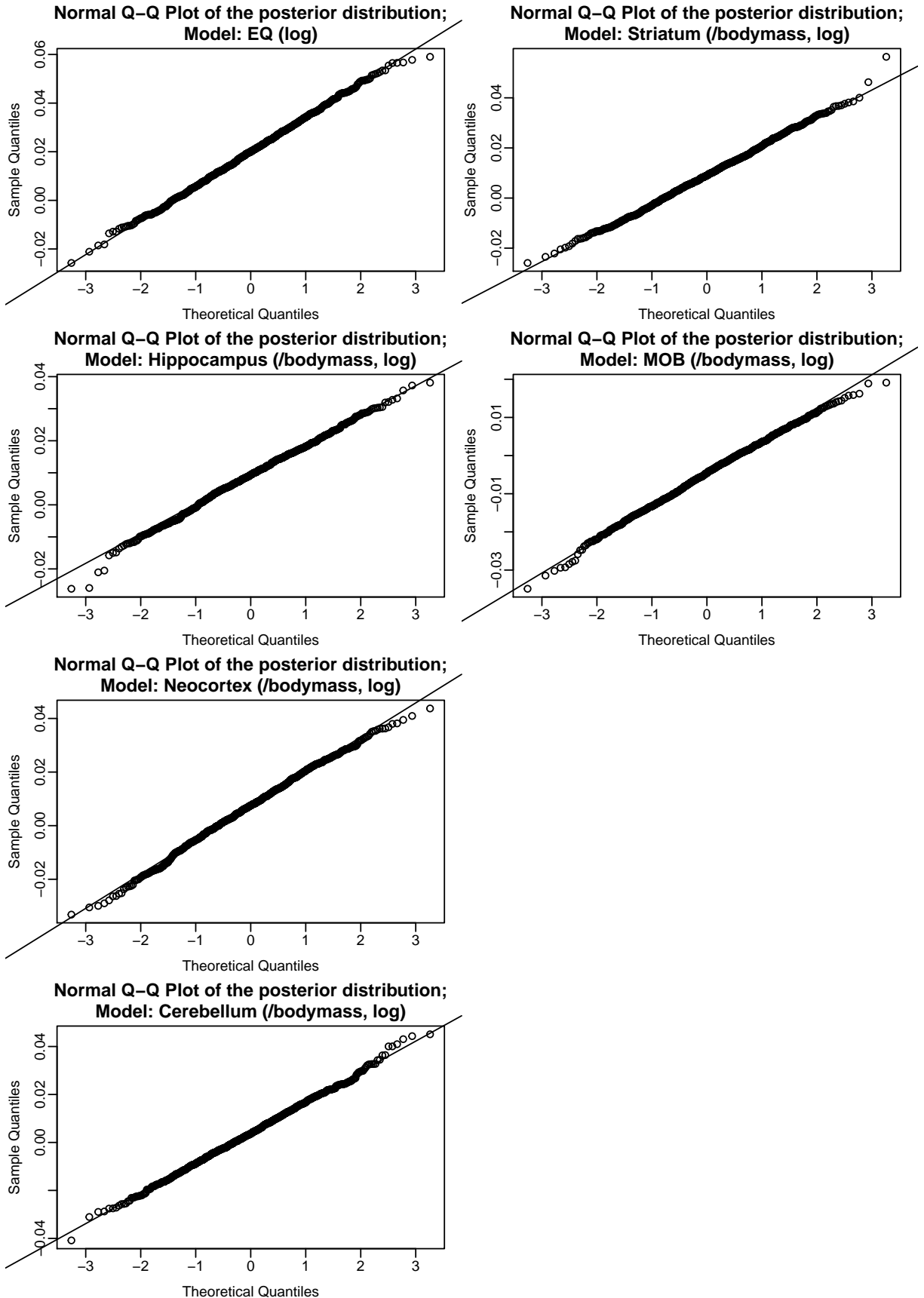


Figure S9: Model assumption check 'Diversity and brain size' | Q-Q plot of the posterior distribution and the expected Gaussian distribution

(b) Phylogenetic regressions: diversification and sympatry

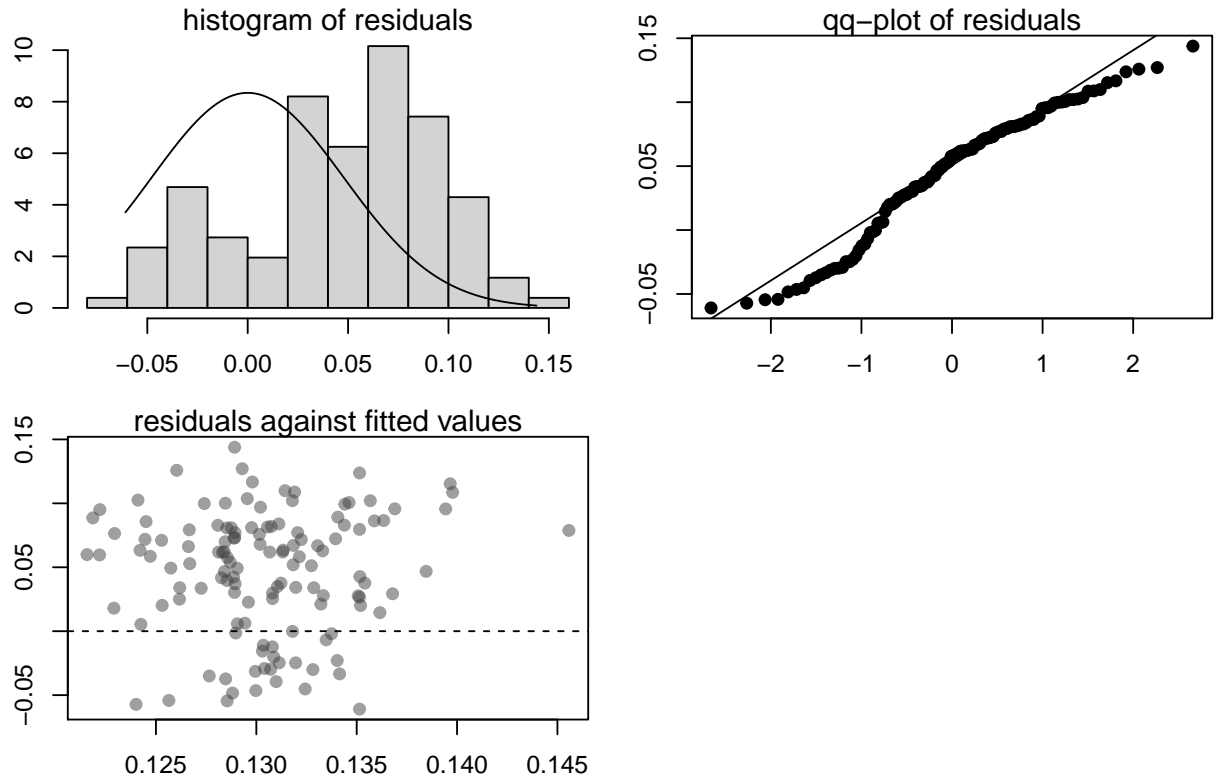


Figure S10: Model assumption check ‘Diversity and sympatry’| Depicted are the histogram of residuals, the Q-Q plot, and the scatter plot of the fitted values *vs* the residuals.

References

1. González-Forero, M. & Gardner, A. Inference of ecological and social drivers of human brain-size evolution. *Nature* **557**, 554–557. ISSN: 14764687 (2018).
2. Navarrete, A., van Schaik, C. P. & Isler, K. Energetics and the evolution of human brain size. *Nature* **480**, 91–93. ISSN: 00280836 (2011).
3. Byrne, R. W. Evolution of primate cognition. *Cognitive Science* **24**, 543–570. ISSN: 03640213 (2000).
4. Byrne, R. W. *Machiavellian intelligence retrospective* **4**, 432–436 (Oxford University Press Oxford, 2018).
5. Dunbar, R. I. & Shultz, S. Why are there so many explanations for primate brain evolution? *Philosophical Transactions of the Royal Society B: Biological Sciences* **372**, 20160244. ISSN: 14712970 (2017).
6. Wilson, A. in *Perspectives on cellular regulation: from bacteria to cancer* 331–340 (J. Wiley & Sons, 1991).

7. Whiten, A. & van Schaik, C. P. The evolution of animal 'cultures' and social intelligence. *Philosophical Transactions of the Royal Society B: Biological Sciences* **362**, 603–620. ISSN: 09628436 (2007).
8. Reader, S. M. & Laland, K. N. Social intelligence, innovation, and enhanced brain size in primates. *Proceedings of the National Academy of Sciences of the United States of America* **99**, 4436–4441. ISSN: 00278424 (2002).
9. Herrmann, E., Call, J., Hernández-Lloreda, M. V., Hare, B. & Tomasello, M. Humans have evolved specialized skills of social cognition: The cultural intelligence hypothesis. *Science* **317**, 1360–1366. ISSN: 00368075 (2007).
10. Tomasello, M. *The cultural origins of human cognition* (Harvard university press, 2019).
11. Van Schaik, C. P. & Burkart, J. M. Social learning and evolution: The cultural intelligence hypothesis. *Philosophical Transactions of the Royal Society B: Biological Sciences* **366**, 1008–1016. ISSN: 14712970 (2011).
12. Ashton, B. J., Kennedy, P. & Radford, A. N. Interactions with conspecific outsiders as drivers of cognitive evolution. *Nature Communications* **11**, 1–9. ISSN: 20411723 (2020).
13. Clutton-Brock, T. H. & Harvey, P. H. Primates, brains and ecology. *Journal of Zoology* **190**, 309–323. ISSN: 14697998 (1980).
14. Milton, K. Distribution Patterns of Tropical Plant Foods as an Evolutionary Stimulus to Primate Mental Development. *American Anthropologist* **83**, 534–548. ISSN: 0002-7294 (1981).
15. Rosati, A. G. Foraging cognition: Reviving the Ecological Intelligence Hypothesis. *Trends in Cognitive Sciences* **21**, 691–702. ISSN: 1879307X (2017).
16. Logan, C. J. *et al.* Beyond brain size: Uncovering the neural correlates of behavioral and cognitive specialization. *Comparative Cognition and Behavior Reviews* **13**, 55–90. ISSN: 19114745 (2018).
17. Barton, R. A. & Harvey, P. H. Mosaic evolution of brain structure in mammals. *Nature* **405**, 1055–1058 (2000).
18. Báez-Mendoza, R. & Schultz, W. The role of the striatum in social behavior. *Frontiers in Neuroscience* **7**, 233. ISSN: 1662453X (2013).
19. Heymann, E. W. & Hsia, S. S. Unlike fellows—a review of primate–non-primate associations. *Biological Reviews* **90**, 142–156 (2015).
20. Johnson, A., van der Meer, M. A. & Redish, A. D. Integrating hippocampus and striatum in decision-making. *Current Opinion in Neurobiology* **17**, 692–697. ISSN: 09594388 (2007).
21. Burgess, N., Maguire, E. A. & O'Keefe, J. The human hippocampus and spatial and episodic memory. *Neuron* **35**, 625–641. ISSN: 08966273 (2002).
22. Janmaat, K. R. *et al.* Spatio-temporal complexity of chimpanzee food: How cognitive adaptations can counteract the ephemeral nature of ripe fruit. *American Journal of Primatology* **78**, 626–645. ISSN: 10982345 (2016).
23. Robira, B., Benhamou, S., Bayanga, E. O., Breuer, T. & Masi, S. Fruits and young leaves in tropical forest: How easy are they to find for western gorillas? (in prep.).
24. Koziol, L. F. *et al.* Consensus paper: The cerebellum's role in movement and cognition. *Cerebellum* **13**, 151–177. ISSN: 14734230 (2014).

25. Sokolov, A. A., Miall, R. C. & Ivry, R. B. The cerebellum: Adaptive prediction for movement and cognition. *Trends in Cognitive Sciences* **21**, 313–332. ISSN: 1879307X (2017).
26. Wiltgen, B. J., Brown, R. A., Talton, L. E. & Silva, A. J. New circuits for old memories: The role of the neocortex in consolidation. *Neuron* **44**, 101–108. ISSN: 08966273 (2004).
27. Grove, M. The evolution of spatial memory. *Mathematical Biosciences* **242**, 25–32. ISSN: 00255564 (2013).
28. Raichle, M. E. *et al.* The brain's dark energy. *Science-New York Then Washington* **314**, 1249 (2006).
29. Laland, K. N. Social learning strategies. *Learning and Behavior* **32**, 4–14. ISSN: 15434494 (2004).
30. Heymann, E. W. & Buchanan-Smith, H. M. The behavioural ecology of mixed-species troops of callitrichine primates. *Biological Reviews* **75**, 169–190. ISSN: 1469185X (2000).
31. Matzke, N. J. Probabilistic historical biogeography: new models for founder-event speciation, imperfect detection, and fossils allow improved accuracy and model-testing. *Frontiers of Biogeography* **5**, na. ISSN: 1948-6596 (2013).
32. Matzke, N. J. Stochastic mapping under biogeographical models. *PhyloWiki Bio-GeoBEARS* **na**, na (2016).
33. Kamilar, J. M. Environmental and geographic correlates of the taxonomic structure of primate communities. *American Journal of Physical Anthropology* **139**, 382–393. ISSN: 00029483 (2009).
34. Bollback, J. P. SIMMAP: Stochastic character mapping of discrete traits on phylogenies. *BMC Bioinformatics* **7**, 1–7. ISSN: 14712105 (2006).
35. Nuismer, S. L. & Harmon, L. J. Predicting rates of interspecific interaction from phylogenetic trees. *Ecology Letters* **18**, 17–27. ISSN: 14610248 (2015).
36. Drury, J., Clavel, J., Manceau, M. & Morlon, H. Estimating the effect of competition on trait evolution using maximum likelihood inference. *Systematic Biology* **65**, 700–710. ISSN: 1076836X (2016).
37. Blomberg, S. P., Rathnayake, S. I. & Moreau, C. M. Beyond brownian motion and the ornstein-uhlenbeck process: Stochastic diffusion models for the evolution of quantitative characters. *American Naturalist* **195**, 145–165. ISSN: 00030147 (2020).
38. Blomberg, S. P., Garland, T. & Ives, A. R. Testing for phylogenetic signal in comparative data: Behavioral traits are more labile. *Evolution* **57**, 717–745. ISSN: 00143820 (2003).
39. Burnham, K. P. & Anderson, D. R. *Model selection and multimodel inference: A practical Information-theoretic approach* Second (Springer, New York, 2002).
40. Isler, K. & van Schaik, C. P. The Expensive Brain: A framework for explaining evolutionary changes in brain size. *Journal of Human Evolution* **57**, 392–400. ISSN: 00472484 (2009).
41. IUCN. *The IUCN Red List of Threatened Species* Downloaded on the 19/01/2021 (2021). <https://www.iucnredlist.org>.
42. Maliet, O., Hartig, F. & Morlon, H. A model with many small shifts for estimating species-specific diversification rates. *Nature Ecology and Evolution* **3**, 1086–1092. ISSN: 2397334X (2019).
43. Maliet, O. & Morlon, H. Fast and accurate estimation of species-specific diversification rates using data augmentation. *Systematic Biology*. ISSN: 1063-5157 (2021).

44. Melchionna, M. *et al.* Macroevolutionary trends of brain mass in Primates. *Biological Journal of the Linnean Society* **129**, 14–25. ISSN: 10958312 (2020).
45. DeCasien, A. R., Williams, S. A. & Higham, J. P. Primate brain size is predicted by diet but not sociality. *Nature Ecology and Evolution* **1**, 1–7. ISSN: 2397334X (2017).
46. Sayol, F., Lapiedra, O., Ducatez, S. & Sol, D. Larger brains spur species diversification in birds. *Evolution* **73**, 2085–2093. ISSN: 15585646 (2019).
47. Sol, D., Székely, T., Liker, A. & Lefebvre, L. Big-brained birds survive better in nature. *Proceedings of the Royal Society B: Biological Sciences* **274**, 763–769. ISSN: 14712970 (2007).
48. Condamine, F. L., Rolland, J. & Morlon, H. Assessing the causes of diversification slowdowns: temperature-dependent and diversity-dependent models receive equivalent support. *Ecology Letters* **22**, 1900–1912. ISSN: 14610248. <https://onlinelibrary.wiley.com/doi/full/10.1111/ele.13382> (Nov. 2019).
49. Kennedy, J. D., Price, T. D., Fjeldså, J. & Rahbek, C. Historical limits on species co-occurrence determine variation in clade richness among New World passerine birds. *Journal of Biogeography* **44**, 736–747. ISSN: 13652699 (2017).
50. Powell, L. E., Isler, K. & Barton, R. A. Re-evaluating the link between brain size and behavioural ecology in primates. *Proceedings of the Royal Society B: Biological Sciences* **284**, 20171765. ISSN: 14712954 (2017).
51. de Almeida Rocha, J. M., Pinto, M. P., Boubli, J. P. & Viveiros Grelle, C. E. The role of competition in structuring primate communities under different productivity regimes in the amazon. *PLoS ONE* **10**, e0145699. ISSN: 19326203 (2015).
52. Suwanvecho, U. & Brockelman, W. Y. Interspecific territoriality in gibbons (*Hylobates lar* and *H. pileatus*) and its effects on the dynamics of interspecies contact zones. *Primates* **53**, 97–108. ISSN: 00328332 (2012).
53. Rafacz, M. & Templeton, J. J. Environmental unpredictability and the value of social information for foraging starlings. *Ethology* **109**, 951–960. ISSN: 01791613 (2003).
54. Dunlap, A. S., Nielsen, M. E., Dornhaus, A. & Papaj, D. R. Foraging bumble bees weigh the reliability of personal and social information. *Current Biology* **26**, 1195–1199. ISSN: 09609822 (2016).
55. Robira, B., Benhamou, S., Masi, S., Llaurens, V. & Riotte-Lambert, L. Foraging efficiency in temporally predictable environments: Is a long-term temporal memory really advantageous? *Royal Society Open Science* (2021).
56. Moen, D. & Morlon, H. Why does diversification slow down? *Trends in Ecology and Evolution* **29**, 190–197. ISSN: 01695347 (2014).
57. Price, T. D. & Kirkpatrick, M. Evolutionarily stable range limits set by interspecific competition. *Proceedings of the Royal Society B: Biological Sciences* **276**, 1429–1434. ISSN: 14712970 (2009).
58. Pigot, A. L. & Tobias, J. A. Species interactions constrain geographic range expansion over evolutionary time. *Ecology Letters* **16**, 330–338. ISSN: 14610248 (2013).
59. Deaner, R. O., Nunn, C. L. & van Schaik, C. P. Comparative tests of primate cognition: Different scaling methods produce different results. *Brain, Behavior and Evolution* **55**, 44–52. ISSN: 00068977 (2000).
60. Healy, S. D. & Rowe, C. A critique of comparative studies of brain size. *Proceedings of the Royal Society B: Biological Sciences* **274**, 453–464. ISSN: 14712970 (2007).

61. Milham, M. P. *et al.* An open resource for non-human primate imaging. *Neuron* **100**, 61–74 (2018).
62. Altschul, D. M. *et al.* Establishing an infrastructure for collaboration in primate cognition research. *PLoS ONE* **14**, e0223675. ISSN: 19326203 (2019).
63. Janmaat, K. R. *et al.* Using natural travel paths to infer and compare primate cognition in the wild. *iScience* **24**, 102343. ISSN: 25890042 (2021).
64. Porter, L. M. Benefits of polyspecific associations for the Goeldi's monkey (*Callimico goeldii*). *American Journal of Primatology* **54**, 143–158. ISSN: 02752565 (2001).
65. Drury, J. P., Cowen, M. C. & Grether, G. F. Competition and hybridization drive interspecific territoriality in birds. *Proceedings of the National Academy of Sciences of the United States of America* **117**, 12923–12930. ISSN: 10916490 (2020).
66. Losin, N., Drury, J. P., Peiman, K. S., Storch, C. & Grether, G. F. The ecological and evolutionary stability of interspecific territoriality. *Ecology Letters* **19**, 260–267. ISSN: 14610248 (2016).
67. Persson, T., Sauciuc, G. A. & Madsen, E. A. Spontaneous cross-species imitation in interactions between chimpanzees and zoo visitors. *Primates* **59**, 19–29. ISSN: 00328332 (2018).
68. Pepperberg, I. M. Allospecific referential speech acquisition in grey parrots (*Psittacus erithacus*): Evidence for multiple levels of avian vocal imitation. *Imitation in Animals and Artifacts*, 109–131 (2002).
69. Carroll, L. *Through the looking glass* (Macmillan London U.K, 1871).
70. R Core Team. *R: A language and environment for statistical computing* Vienna, Austria, 2020. <http://www.r-project.org%20https://www.r-project.org/>.
71. DeCasien, A. R. & Higham, J. P. Primate mosaic brain evolution reflects selection on sensory and cognitive specialization. *Nature Ecology and Evolution* **3**, 1483–1493. ISSN: 2397334X (2019).
72. Powell, L. E., Barton, R. A. & Street, S. E. Maternal investment, life histories and the evolution of brain structure in primates. *Proceedings of the Royal Society B: Biological Sciences* **286**, 20191608. ISSN: 14712954 (2019).
73. Todorov, O. S., Weisbecker, V., Gilissen, E., Zilles, K. & De Sousa, A. A. Primate hippocampus size and organization are predicted by sociality but not diet. *Proceedings of the Royal Society B: Biological Sciences* **286**, 20191712. ISSN: 14712954 (2019).
74. Grueter, C. C. Home range overlap as a driver of intelligence in primates. *American Journal of Primatology* **77**, 418–424. ISSN: 10982345 (2015).
75. Navarrete, A. F. *et al.* Primate Brain Anatomy: New Volumetric MRI Measurements for Neuroanatomical Studies. *Brain, Behavior and Evolution* **91**, 109–117. ISSN: 14219743 (2018).
76. Pearce, F., Carbone, C., Cowlshaw, G. & Isaac, N. J. Space-use scaling and home range overlap in primates. *Proceedings of the Royal Society B: Biological Sciences* **280**, 20122122. ISSN: 14712954 (2013).
77. Willems, E. P., Hellriegel, B. & van Schaik, C. P. The collective action problem in primate territory economics. *Proceedings of the Royal Society B: Biological Sciences* **280**, 20130081. ISSN: 14712954 (2013).
78. Bivand, R. & Rundel, C. *rgeos: Interface to Geometry Engine - Open Source ('GEOS')* R package version 0.5-5 (2020). <https://CRAN.R-project.org/package=rgeos>.

79. Hijmans, R. J. *geosphere: Spherical Trigonometry* R package version 1.5-10 (2019). <https://CRAN.R-project.org/package=geosphere>.
80. Pavoine, S., Bonsall, M. B., Davies, T. J. & Masi, S. Mammal extinctions and the increasing isolation of humans on the tree of life. *Ecology and Evolution* **9**, 914–924. ISSN: 20457758 (2019).
81. Pineda-Munoz, S., Wang, Y., Kathleen Lyons, S., Tóth, A. B. & McGuire, J. L. Mammal species occupy different climates following the expansion of human impacts. *Proceedings of the National Academy of Sciences of the United States of America* **118**. ISSN: 10916490 (2021).
82. Masi, S., Cipolletta, C. C. & Robbins, M. M. Western lowland gorillas (*Gorilla gorilla gorilla*) change their activity patterns in response to frugivory. *American Journal of Primatology* **71**, 91–100. ISSN: 02752565 (2009).
83. Revell, L. J. phytools: An R package for phylogenetic comparative biology (*and other things*). *Methods in Ecology and Evolution* **3**, 217–223 (2012).
84. Slater, G. *et al.* Fitting models of continuous trait evolution to incompletely sampled comparative data using approximate Bayesian computation. *Evolution* **66**, 752–762 (2012).
85. Pennell, M. *et al.* geiger v2.0: an expanded suite of methods for fitting macroevolutionary models to phylogenetic trees. *Bioinformatics* **30**, 2216–2218 (2014).
86. Morlon, H. *et al.* RPANDA: an R package for macroevolutionary analyses on phylogenetic trees. *Methods in Ecology and Evolution* **7**. R package version 1.4, 589–597. <https://CRAN.R-project.org/package=RPANDA> (2016).
87. Weir, J. T. & Mursleen, S. Diversity-dependent cladogenesis and trait evolution in the adaptive radiation of the auks (*Aves: Alcidae*). *Evolution* **67**, 403–416. ISSN: 00143820 (2013).
88. Gelman, A. & Rubin, D. B. Inference from iterative simulation using multiple sequences. *Statistical Science* **7**, 457–472. ISSN: 08834237 (1992).
89. Dos Reis, M. *et al.* Using phylogenomic data to explore the effects of relaxed clocks and calibration strategies on divergence time estimation: Primates as a test case. *Systematic Biology* **67**, 594–615. ISSN: 1076836X (2018).
90. Estrada, A. *et al.* Impending extinction crisis of the world’s primates: Why primates matter. *Science Advances* **3**, e1600946. ISSN: 23752548 (2017).
91. Ho, L. S. T. & Ane, C. A linear-time algorithm for Gaussian and non-Gaussian trait evolution models. *Systematic Biology* **63**, 397–408 (2014).
92. Mundry, R. in *Modern Phylogenetic Comparative Methods and their Application in Evolutionary Biology* 131–153 (Springer, 2014). ISBN: 9783662435502.
93. Hadfield, J. D. MCMC Methods for Multi-Response Generalized Linear Mixed Models: The MCMCglmm R Package. *Journal of Statistical Software* **33**, 1–22. <https://www.jstatsoft.org/v33/i02/> (2010).
94. Plummer, M., Best, N., Cowles, K. & Vines, K. CODA: Convergence Diagnosis and Output Analysis for MCMC. *R News* **6**, 7–11. [https://journal.r-project.org/archive/\(2006\)](https://journal.r-project.org/archive/(2006)).
95. Modolo, L., Salzburger, W. & Martin, R. D. Phylogeography of Barbary macaques (*Macaca sylvanus*) and the origin of the Gibraltar colony. *Proceedings of the National*

- Academy of Sciences of the United States of America* **102**, 7392–7397. ISSN: 00278424 (2005).
96. Muschelli, J. *neurobase: 'Neuroconductor' Base Package with Helper Functions for 'nifti' Objects* R package version 1.32.0 (2021). <https://CRAN.R-project.org/package=neurobase>.
 97. Feng, D. & Tierney, L. Computing and Displaying Isosurfaces in R. *Journal of Statistical Software* **28**. <https://www.jstatsoft.org/v28/i01/> (2008).
 98. Zeileis, A., Leisch, F., Hornik, K. & Kleiber, C. strucchange: An R Package for Testing for Structural Change in Linear Regression Models. *Journal of Statistical Software* **7**, 1–38. <http://www.jstatsoft.org/v07/i02/> (2002).
 99. Zeileis, A., Kleiber, C., Krämer, W. & Hornik, K. Testing and Dating of Structural Changes in Practice. *Computational Statistics & Data Analysis* **44**, 109–123 (2003).
 100. Zeileis, A. Implementing a Class of Structural Change Tests: An Econometric Computing Approach. *Computational Statistics & Data Analysis* **50**, 2987–3008 (2006).
 101. Arbour, J. H. & Santana, S. E. A major shift in diversification rate helps explain macroevolutionary patterns in primate species diversity. *Evolution* **71**, 1600–1613. ISSN: 15585646 (2017).
 102. Springer, M. S. *et al.* Macroevolutionary dynamics and historical biogeography of primate diversification inferred from a species supermatrix. *PLoS ONE* **7**, e49521. ISSN: 19326203 (2012).
 103. Fleagle, J. G. & Gilbert, C. C. in *Primate Biogeography* 375–418 (Springer, 2006).